CHAPTER FOUR

Coronavirus *cis*-Acting RNA Elements

R. Madhugiri*, M. Fricke†, M. Marz†,‡, J. Ziebuhr*,1
*Institute of Medical Virology, Justus Liebig University Giessen, Giessen, Germany
†Faculty of Mathematics and Computer Science, Friedrich Schiller University Jena, Jena, Germany
‡FLI Leibniz Institute for Age Research, Jena, Germany
1Corresponding author: e-mail address: john.ziebuhr@viro.med.uni-giessen.de

Contents

Abstract

Coronaviruses have exceptionally large RNA genomes of approximately 30 kilobases. Genome replication and transcription is mediated by a multisubunit protein complex comprised of more than a dozen virus-encoded proteins. The protein complex is thought to bind specific *cis*-acting RNA elements primarily located in the 5′- and 3′-terminal genome regions and upstream of the open reading frames located in the 3′-proximal one-third of the genome. Here, we review our current understanding of coronavirus *cis*-acting RNA elements, focusing on elements required for genome replication and packaging. Recent bioinformatic, biochemical, and genetic studies suggest a previously unknown level of conservation of *cis*-acting RNA structures among different coronavirus genera and, in some cases, even beyond genus boundaries. Also, there is increasing evidence to suggest that individual *cis*-acting elements may be part of higher-order RNA structures involving long-range and dynamic RNA–RNA interactions between RNA structural elements separated by thousands of nucleotides in the viral genome. We discuss the structural and functional features of these *cis*-acting RNA elements and their specific functions in coronavirus RNA synthesis.

Advances in Virus Research, Volume 96
ISSN 0065-3527
http://dx.doi.org/10.1016/bs.aivir.2016.08.007

1. INTRODUCTION

Coronaviruses are enveloped, positive-strand RNA viruses. They have been united in the subfamily *Coronavirinae* within the family *Coronaviridae* (de Groot et al., 2012a; Masters and Perlman, 2013). Together with three other families (*Arteriviridae*, *Roniviridae*, and *Mesoniviridae*), the *Coronaviridae* form the order *Nidovirales* (de Groot et al., 2012b). According to the current classification, the family *Coronaviridae* comprises four genera called *Alpha-*, *Beta-*, *Gamma-*, and *Deltacoronavirus*. In some cases, these genera have been further subdivided into lineages. Coronaviruses infect a wide range of mammals and birds and include pathogens of major medical, veterinary, and economic interest (de Groot et al., 2012a; Fehr and Perlman, 2015; Masters and Perlman, 2013), with severe acute respiratory syndrome (SARS) coronavirus (SARS-CoV), and Middle East respiratory syndrome (MERS) coronavirus (MERS-CoV) providing two prominent examples of zoonotic coronaviruses causing severe respiratory disease in humans (Drosten et al., 2003; Ksiazek et al., 2003; Vijay and Perlman, 2016; Zaki et al., 2012; Zumla et al., 2015).

Among plus-strand RNA viruses, coronaviruses and related nidoviruses stick out by their large genome size of about 30 kilobases (kb), the synthesis of numerous subgenomic mRNAs, and the large number of nonstructural proteins (nsps) involved in viral RNA synthesis and interactions with host cell functions (reviewed in Masters and Perlman, 2013; Ziebuhr, 2008). Most of the nsps are encoded by the viral replicase gene that occupies the 5′-terminal two-thirds of the genome and is comprised of two large open reading frames, ORF1a and ORF1b. Translation of ORF1a yields polyprotein (pp) 1a (~450 kDa). Translation of ORF1b requires a programmed ribosomal frameshift event (Brierley et al., 1987, 1989) that occurs just upstream of the ORF1a stop codon and results in pp1ab (~750 kDa). Co- and posttranslational cleavage of pp1a/1ab by two types of virus-encoded proteases associated with nsp3 and nsp5 (Mielech et al., 2014; Ziebuhr et al., 2000) gives rise to a total of 15–16 mature proteins that form the viral replication–transcription complex (RTC) which is thought to also involve the nucleocapsid protein and several cellular proteins (Almazan et al., 2004; Schelle et al., 2005; Ziebuhr, 2008; Ziebuhr et al., 2000). This multiprotein complex replicates the viral genome and produces an extensive set of 3′-coterminal subgenomic messenger RNAs (sg mRNAs), the latter representing a hallmark of corona- and other nidoviruses (Pasternak et al.,

2006; Sawicki et al., 2007; Ziebuhr and Snijder, 2007). The sg mRNAs are used to express the genes located downstream of the replicase gene, involving the viral structural proteins (nucleocapsid (N), membrane (M), spike (S), and envelope (E) protein) and several accessory proteins that, in many cases, have been implicated in functions that interfere with antiviral host responses (Liu et al., 2014; Masters and Perlman, 2013; Narayanan et al., 2008b).

In this chapter, we will briefly summarize coronavirus RNA synthesis and then discuss the structural and functional features of currently known *cis*-acting RNA elements located in the 5′- and 3′-terminal untranslated regions (UTR) and neighboring coding regions. Also, we will review the current knowledge of signals required for packaging and of cellular proteins presumed to be involved in viral RNA synthesis.

2. CORONAVIRUS GENOME REPLICATION AND TRANSCRIPTION

Following receptor-mediated entry into the host cell, the viral genome RNA, which is 5′-capped and 3′-polyadenylated, is released from the nucleocapsid and used for translation of the 5′-terminal ORFs 1a and 1b to produce the key components of the viral RTC. The complex is anchored by membrane-spanning domains (residing in nsp3, 4, and 6) to virus-induced membranous structures that provide a scaffold for the protein machinery involved in viral RNA synthesis (den Boon and Ahlquist, 2010; Gosert et al., 2002; Kanjanahaluethai et al., 2007; Knoops et al., 2008; Oostra et al., 2007, 2008; Snijder et al., 2006; van Hemert et al., 2008). Over the past years, a wealth of information has been obtained on enzymatic and other functions, three-dimensional structures and interactions of individual nsps produced from pp1a and pp1ab (reviewed in Imbert et al., 2010; Masters, 2006; Ulferts et al., 2010; Ziebuhr, 2008). The studies show that, in addition to common enzymes conserved in most +RNA viruses, such as RNA-dependent RNA polymerase (RdRp) (te Velthuis et al., 2010), helicase/NTPase (Seybert et al., 2000), proteases (Baker et al., 1989; Ziebuhr et al., 1995), 5′ cap-specific methylases (Chen et al., 2009b; Decroly et al., 2008, 2011), coronaviruses encode an extra set of proteins in their replicase genes. These additional (sometimes even unique) enzymatic functions include a 3′–5′ exoribonuclease (Minskaia et al., 2006; Snijder et al., 2003) that is thought to be involved in mechanisms required for high-fidelity replication of nidovirus (including coronavirus) genomes of more than 20 kb (Eckerle et al., 2010; Minskaia et al., 2006; Smith et al., 2013, 2014) and a

uridylate-specific endoribonuclease of currently unknown function that was found to be conserved in all vertebrate nidoviruses (Ivanov et al., 2004; Nga et al., 2011; Ulferts and Ziebuhr, 2011). In some cases, the replicase gene-encoded enzymes could be linked to specific steps of viral RNA synthesis and/or RNA processing or were shown to interfere with cellular functions (reviewed in Fehr and Perlman, 2015; Masters and Perlman, 2013; Ziebuhr, 2008). Interactions between different nsps have been predicted and characterized for a large number of proteins and the structural basis and possible functional implications of these interactions has been a major topic of research. For example, it has been shown that the exoribonuclease and ribose 2′-*O*-methyltransferase activities associated with nsp14 and nsp16, respectively, are stimulated by nsp10 and the interacting surfaces have been identified by mutagenesis and structural studies (Bouvet et al., 2014; Decroly et al., 2011; Ma et al., 2015). Also, there is evidence that a hexadecameric complex formed by eight molecules of nsp7 and eight molecules of nsp8 assists the RdRp by acting as a processivity factor (Subissi et al., 2014; Zhai et al., 2005). Additional interactions between individual subunits of the RTC have been suggested on the basis of two-hybrid screening data (Pan et al., 2008; von Brunn et al., 2007) and there is evidence that a large number of coronavirus nsps assemble to form homo- or heterooligomeric complexes (Anand et al., 2002, 2003; Bouvet et al., 2014; Chen et al., 2011; Ma et al., 2015; Ricagno et al., 2006; Su et al., 2006; Xiao et al., 2012; Zhai et al., 2005).

Coronaviruses produce a set of 5′- and 3′-coterminal sg mRNAs that contain a common 5′-leader sequence of about 60–95 nt (Spaan et al., 1983). The sequence of this leader is identical to the 5′-terminal sequence of the viral genome RNA. Synthesis of coronavirus sg mRNAs is thought to involve a "discontinuous" step during negative-strand RNA synthesis (Sawicki and Sawicki, 1995). Specific proteins of the RTC that are required for (or involved in) this discontinuous extension step remain to be identified while important *cis*-acting RNA elements, called "transcription-regulating sequences" (TRSs), that are required for this step have been characterized for a number of coronaviruses (reviewed in Sola et al., 2011b, 2015). TRSs are located downstream of the 5′-leader on the genome ("leader-TRS," TRS-L) and upstream of each of the major ORFs present in the 3′-proximal genome region ("body-TRSs," TRS-B). They play a vital role in supporting the transfer of the nascent minus strand from a distant position in the 3′-proximal genome region to the TRS-L located near the 5′-end of the genome following attenuation of

minus-strand RNA synthesis at one of the TRS-B. Coronavirus TRSs contain an AU-rich motif of about 10 nucleotides that is involved in base-pairing interactions between the TRS-L and the complement of a body-TRS (Sawicki and Sawicki, 1995, 1998; Sawicki et al., 2007; Sethna et al., 1991). Following transfer of the nascent minus strand from its downstream position on the template (at the TRS-B) to the TRS-L close to the 5′ end of the genome, negative-strand RNA synthesis is resumed and completed by copying the 5′ leader sequence. The resulting set of 3′ antileader-containing sg minus-strand RNAs is subsequently used as templates for the production of the characteristic nested set of 5′ leader-containing mRNAs in coronavirus-infected cells (Lai et al., 1983; Sawicki and Sawicki, 1995; Sawicki et al., 2001; Sethna et al., 1989; Spaan et al., 1983). Sg minus-strand RNAs contain a U-stretch at their 5′ end, providing a possible template for 3′ polyadenylation of sg mRNAs (Hofmann and Brian, 1991; Wu et al., 2013).

As mentioned earlier, the *cis*-acting RNA elements required for coronavirus replication (and transcription) are located in the 5′- and 3′-terminal genome regions and largely (but not exclusively) encompass noncoding regions (Chang et al., 1994; Dalton et al., 2001; Izeta et al., 1999; Kim et al., 1993; Liao and Lai, 1994; Lin et al., 1994, 1996; Zhang et al., 1994). Additional *cis*-acting elements are located at internal positions and include the TRS elements involved in transcription as well as specific RNA signals required for genome packaging (Chen et al., 2007; Escors et al., 2003; Makino et al., 1990; Morales et al., 2013; Penzes et al., 1994). Another important RNA structural element is located in the ORF1a–ORF1b overlap region. This complex pseudoknot structure mediates a (−1) ribosomal frameshift event and thus controls the expression of the second large ORF on the coronavirus genome RNA (ORF1b) (Brierley et al., 1987, 1989; de Haan et al., 2002; Namy et al., 2006).

3. CORONAVIRUS *cis*-ACTING RNA ELEMENTS

Historically, *cis*-acting RNA elements essential for coronavirus RNA synthesis have mainly been characterized using naturally occurring and genetically engineered defective interfering RNAs (DI RNAs) (reviewed in Brian and Baric, 2005; Brian and Spaan, 1997; Masters, 2007; Sola et al., 2011b). DI RNAs are relatively short RNAs that are derived from viral genome RNA but lack large (internal) sequence parts. DI RNAs are replicated in cells provided that a suitable (i.e., closely related) helper virus

provides functional replicase complexes *in trans* (Levis et al., 1986; Weiss et al., 1983) and that the DI RNA contains all the *cis*-acting RNA signals required for replication. In general, DI RNAs contain the entire 5′- and 3′-untranslated genome regions and, in most cases, also small parts of neighboring (or internal) coding regions (Lin and Lai, 1993). Coronavirus DI RNAs were first reported and most extensively studied for the betacoronaviruses MHV and BCoV (Chang et al., 1994; de Groot et al., 1992; Hofmann et al., 1990; Luytjes et al., 1996; Makino et al., 1984, 1985, 1988a,b). Subsequently, DI RNAs were also identified and characterized in alpha- and gammacoronaviruses (Izeta et al., 1999; Mendez et al., 1996; Penzes et al., 1994, 1996).

Identification and characterization of DI RNAs in various coronaviruses have been instrumental in mapping the minimal RNA sequences and structures required for replication and packaging. A major problem in studies using DI RNAs for defining elements required for replication was the high-frequency homologous recombination between the RNA replicon and the helper virus genome. For example, BCoV-derived artificial DI RNAs containing base substitutions within 5′ leader sequences rapidly acquired the leader sequence of the helper virus (Chang et al., 1994, 1996; Makino and Lai, 1990). This "leader switching" was regularly observed in serial passaging experiments aimed to rescue (or amplify) DI RNAs for further phenotypic characterization. With the development of a range of coronavirus reverse genetic systems, the manipulation of full-length coronavirus cDNA copies for functional characterization of *cis*-acting RNA elements at the genome level (including long-range RNA–RNA interactions) has now become an attractive alternative to overcome some of the limitations of the DI RNA-based systems used previously (Almazan et al., 2000; Casais et al., 2001; Scobey et al., 2013; Tekes et al., 2008; Thiel et al., 2001; van den Worm et al., 2012; Yount et al., 2000, 2003).

3.1 5′-Terminal *cis*-Acting RNA Elements

DI RNA-based studies performed with representative betacoronaviruses (MHV and BCoV) revealed that approximately 500 nt from the genomic 5′ end (467 nt in MHV and 498 nt in BCoV) are required for replication (Chang et al., 1994; Kim et al., 1993; Luytjes et al., 1996). Similar 5′-terminal sequence requirements were established in subsequent studies for the alphacoronavirus TGEV (649 nt) (Escors et al., 2003) and the gammacoronavirus IBV (544 nt) (Dalton et al., 2001). These DI RNAs

contained the entire 5′ UTR, ranging in size from 210 nt (MHV, BCoV, and HCoV-OC43) to 314 nt (TGEV), and a part of the replicase gene (from the nsp1-coding region) (see later). In contrast to alpha- and betacoronaviruses, the gammacoronavirus IBV features a larger 5′ UTR (528 nt) (Boursnell et al., 1987) and lacks an equivalent of nsp1 (Ziebuhr et al., 2001). In this case, the 5′ UTR alone appears to contain all the signals required for genome replication.

3.1.1 Structural Features of Coronavirus 5′-Terminal cis-Acting Elements

The majority of the 5′-proximal RNA structures and sequences essential for coronavirus genome replication have first been characterized for BCoV using DI RNA-based systems (Brown et al., 2007; Chang et al., 1994, 1996; Gustin et al., 2009; Raman and Brian, 2005; Raman et al., 2003). The 5′-proximal 215 nts of the BCoV genome were predicted to harbor four stem-loops (SLs) that, in the older literature, were termed SL I (comprised of Ia and Ib), II, III, and IV. The structures were identified by in vitro structure probing analysis of appropriate DI RNAs and their *cis*-acting functions were investigated by DI RNA replication studies and mutation analysis. More recently, two additional SLs called SL-V and SL-VI were identified in the BCoV nsp1-coding region, with SL-VI being essential for DI RNA replication (Brown et al., 2007).

Unlike BCoV, MHV is predicted to contain three conserved SLs, SL1, SL2, and SL4, in this 5′-terminal genome region (Fig. 1). Using 5′-terminal genome sequences of about 140 nts of nine coronaviruses, including five betacoronaviruses (BCoV, human coronavirus (HCoV) OC43, HCoV-HKU1, SARS-CoV, and MHV-A59), three alphacoronaviruses (HCoV-NL63, HCoV-229E, and TGEV), and one gammacoronavirus (IBV), the Leibowitz and Giedroc laboratories proposed a consensus 5′-terminal RNA secondary structure model (Kang et al., 2006; Liu et al., 2007) that includes three highly conserved hairpin structures, SL1, SL2, and SL4. This model was confirmed and extended by genus-wide alignment-based secondary structure predictions using LocARNA (Madhugiri et al., 2014; Smith et al., 2010; Will et al., 2007, 2012) in which, despite profound sequence diversity in this genome region, three highly conserved SLs SL1, SL2, and SL4 were identified in the 5′-terminal 150-nt betacoronavirus genome regions (Madhugiri et al., 2014) (Fig. 1).

Interestingly, the BCoV and SARS-CoV genome RNAs were predicted to accommodate an additional SL (called SL3) in the region between SL2

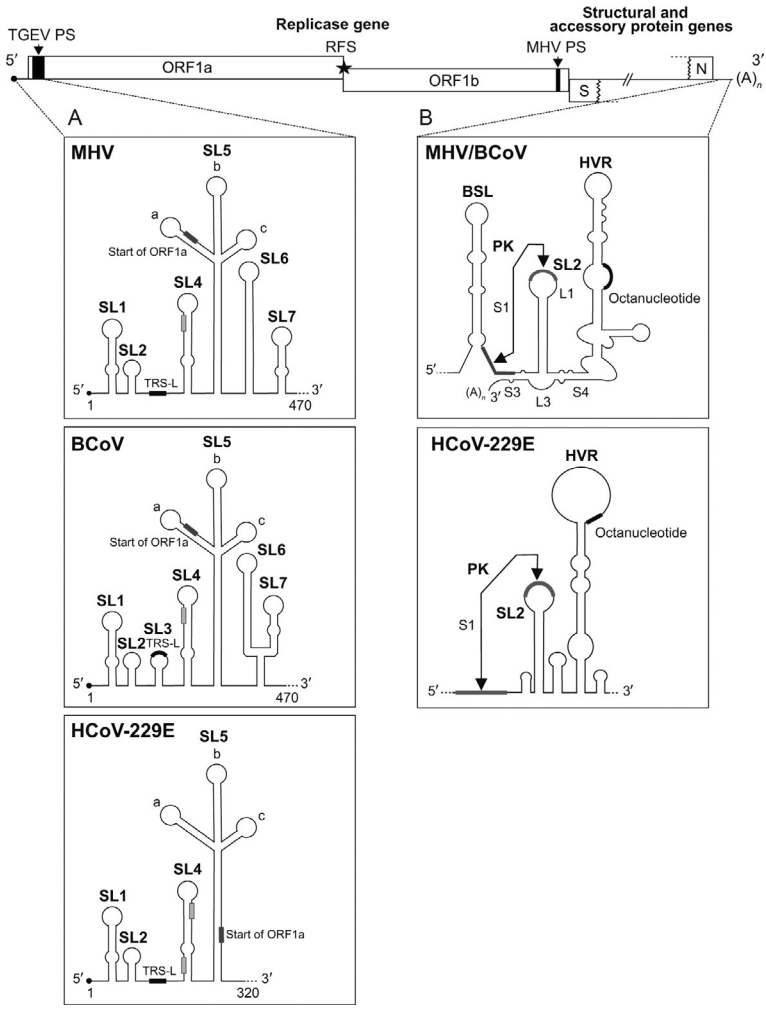

Fig. 1 Conserved *cis*-acting RNA elements in the 5′- and 3′-proximal genome regions of coronaviruses. Shown is the coronavirus genome organization with the two large 5′ ORFs, 1a and 1b, that together constitute the replicase gene, while details of structural and accessory protein ORFs are not shown. *Black circles* at the RNA 5′ ends indicate the 5′ cap structure, while $(A)_n$ indicates the 3′ poly(A) tail. The −1 ribosomal frameshift signal (RFS) at the ORF1a/1b junction site is indicated by an asterisk. *S*, S gene; *N*, N gene. Approximate positions of the packaging signals (PS) determined for MHV and TGEV are indicated by *arrows*. (A) Schematic representation of RNA structural elements in the 5′-terminal genome regions of MHV, BCoV, and HCoV-229E. *Filled boxes* indicate the leader-TRS (TRS-L). *Boxes* in *light gray* indicate the start codons of the uORF(s) located upstream of ORF1a. *Boxes* in *dark gray* indicate the position of the ORF1a start codon. (B) Schematic representation of RNA structural elements in the 3′-terminal genome regions of MHV, BCoV, and HCoV-229E. Major conserved RNA structural elements are shown, together with base-pairing interactions required to form a pseudoknot (PK) structure. Also shown is the position of a highly conserved octanucleotide sequence that is located in a single-stranded region. *BSL*, bulged stem-loop; *L*, loop; *S*, stem; *SL*, stem-loop structure; *HVR*, hypervariable region; *PK*, pseudoknot.

and SL4. SL3 is predicted to adopt a stable hairpin structure containing the TRS-L (Fig. 1). The formation of an equivalent SL3 structure can also be forced for MHV and several other betacoronaviruses (Chen and Olsthoorn, 2010; Madhugiri et al., 2014), although this structural element would only contain two conserved base pairs and was predicted to be unstable at 37°C (Liu et al., 2007). In a recent study, we extended these studies and used multiple alignments calculated with LocARNA (Madhugiri et al., 2014; Smith et al., 2010; Will et al., 2007, 2012) to identify conserved RNA structural elements conserved in the 5′-proximal genome regions of alphacoronaviruses (Madhugiri et al., 2014). The predicted structures were verified and refined by RNA structure probing analyses (Ehresmann et al., 1987; Qu et al., 1983) using in vitro-transcribed RNAs with sequences corresponding to the 5′-terminal genome regions of HCoV-229E and HCoV-NL63, respectively. The combined structural and phylogenetic analyses performed in different laboratories produce a rather coherent picture, with SL1, SL2, and SL4 representing *cis*-acting RNA elements that are highly conserved across different coronavirus genera despite pronounced sequence diversity in the respective 5′-terminal genome regions (Chen and Olsthoorn, 2010; Kang et al., 2006; Liu et al., 2007; Madhugiri et al., 2014).

To further confirm the previously identified conserved betacoronavirus 5′-proximal RNA secondary structures, a recent study used a selective 2′-hydroxyl acylation and primer extension (SHAPE) methodology to determine the secondary structure of the 5′-terminal 474 nts region of the MHV-A59 genome RNA in the virus (in virio), after gentle extraction and deproteinization (ex virio) and an in vitro-transcribed RNA (Yang et al., 2015). With very few exceptions, the RNA secondary structures determined in this study essentially confirmed the previously characterized or predicted SL1, SL2, and SL4 structures (Fig. 1) (Li et al., 2008; Liu et al., 2007, 2009; Yang et al., 2011). The SHAPE analyses also confirmed that the (weak) TRS-L-containing SL3 hairpin predicted previously by phylogenetic algorithms (Chen and Olsthoorn, 2010) is part of a single-stranded region, consistent with previous predictions that this region is weekly paired or unpaired (Liu et al., 2007; Madhugiri et al., 2014). Also several other RNA secondary structures identified by SHAPE analysis corresponded very well to the previous models of MHV-A59 RNA secondary structures proposed by Brian and coworkers (Guan et al., 2011, 2012; Yang et al., 2015). Furthermore, the study provides biochemical support for the presence of additional hairpin structures in the MHV 5′-terminal genome region,

including SL5a (designated earlier as SL-IV), SL5b, SL5c, SL6, and SL7. An *Alphacoronavirus* genus-wide bioinformatics study revealed a very well conserved higher-order RNA structure (comprising 5a, 5b, and 5c) in an equivalent genome region (Madhugiri et al., 2014). The predicted SL5a, b, and c structures were confirmed and refined by in vitro RNA structure probing information obtained for the 5′-terminal 600 nts of HCoV-229E and HCoV-NL63 (Madhugiri et al., 2014; unpublished data). Also, the study identified significant constraints in the alphacoronavirus SL5 as judged by the large number of covariant base pairs, suggesting an important function in alphacoronavirus RNA synthesis, possibly related to that described for the betacoronavirus MHV-A59 SL-IV (=SL5a) in supporting efficient viral replication. Furthermore, SL5 was suggested to be involved in long-range RNA–RNA interactions (Guan et al., 2012), which was found to be in good agreement with the SHAPE analysis data (Yang et al., 2015).

Downstream of SL5, additional SL structures (SL6, 7, and 8) were identified. The available evidence suggests that these structures are less well conserved among MHV, BCoV, and SARS-CoV and probably play a less important role in viral replication (Brockway and Denison, 2005; Yang et al., 2015).

Taken together, the available information suggests a model in which the 5′-terminal ~320-nt genome regions of both alpha- and betacoronaviruses contain four major RNA structural elements called SL1, SL2, SL4, and SL5 (Chen and Olsthoorn, 2010; Kang et al., 2006; Liu et al., 2007; Madhugiri et al., 2014; Yang et al., 2015) (see Fig. 1). The conservation of the SL1, SL2, SL4, and SL5abc RNA structural elements (despite pronounced nucleotide sequence divergency) suggests important functions for these structures in the coronavirus life cycle. Functional features of individual structural elements will be discussed later in more detail.

3.1.2 Functional Roles of Coronavirus 5′-Terminal cis-Acting Elements

In contrast to the growing body of information on structures and their conservation in the coronavirus 5′-terminal genome region across all genera of coronaviruses, the functional significance of the individual SL structures has almost exclusively been studied for two (closely related) betacoronaviruses, MHV and BCoV. The structural and functional conservation inferred from these studies for 5′-terminal betacoronavirus *cis*-acting elements was substantiated by reverse genetic data demonstrating that SARS-CoV SL1, SL2, and SL4 can functionally replace their counterparts in the MHV

genome when introduced individually (Kang et al., 2006). Unlike the individual hairpin structure substitution, replacement of the entire MHV 5′ UTR with that of SARS-CoV did not yield a viable MHV mutant, possibly indicating a requirement for stable or transient long-range RNA–RNA interactions of the 5′ UTR with other genome regions. Evidence to support this hypothesis was obtained in subsequent studies. For example, the energetically unstable lower part of MHV SL1 was found to be involved in long-range RNA interactions with the 3′ UTR (Li et al., 2008) (see later). Similar to the SARS-CoV data mentioned earlier, each of the four BCoV 5′-terminal SLs, SL1, SL2, SL4, and SL5a, was shown to functionally replace its MHV counterpart, yielding chimeric viruses with near-wild-type replication kinetics. Furthermore, using MHV/BCoV chimera, a region downstream of SL5 was revealed to be engaged in long-range interactions with the nsp1-coding region, possibly forming an extensive higher-order RNA structure (Guan et al., 2012). Furthermore, a mutagenesis study using BCoV DI RNA (Su et al., 2014) indicated that this multipartite RNA structure may involve several SL substructures identified in earlier studies (Gustin et al., 2009; Raman and Brian, 2005) but require refolding of other RNA structures suggested earlier to be essential for DI RNA replication (Brown et al., 2007). A recent study (Su et al., 2014) provided evidence that a short oligopeptide from the N-terminal domain of nsp1 may be an essential *cis*-acting protein factor involved in betacoronavirus replication, thus adding to the multiple other functions of this protein (Brockway and Denison, 2005; Huang et al., 2011a,b; Kamitani et al., 2006, 2009; Lei et al., 2013; Lokugamage et al., 2012; Narayanan et al., 2008a; Tanaka et al., 2012; Tohya et al., 2009; Wathelet et al., 2007; Züst et al., 2007).

3.1.2.1 Stem-Loops 1 and 2

The 5′-proximal SL1 and SL2 are predicted to be conserved across all genera of the *Coronavirinae* (Chen and Olsthoorn, 2010; Liu et al., 2007). Nuclear magnetic resonance spectroscopy studies of MHV and HCoV-OC43 SL1 RNAs revealed a functionally and structurally bipartite structure for this SL (Li et al., 2008). SL1 was proposed to exist in an equilibrium with higher-energy (partially unfolded) conformers. Characterization of MHV mutants containing specific replacements in SL1 and sequence analysis of second-site revertants support a "dynamic SL1" model in which the lower part of SL1 is required to have an optimally balanced stability/lability. The structural destabilization of the upper part of SL1 by disrupting specific base-pair interactions proved to be lethal or resulted in viruses with replication defects,

while compensatory mutations that restored the base pairing in the upper part of SL1 restored viral replication to near-wild-type levels, suggesting that efficient virus replication requires this part of SL1 to be base-paired. In contrast, disruption of the basal part of SL1 was largely tolerated while compensatory mutations that restored base pairing in the lower part proved to be lethal, suggesting a prominent role for RNA sequence rather than structure conservation in the lower part of SL1. Interestingly, the study also identified a possible link between SL1 and minus-strand subgenomic RNA synthesis (Li et al., 2008). The combined data presented in this study suggest that SL1 requires an optimized stability suitable to establish or fine-tune transient long-range (RNA- or protein-mediated) interactions between the 5′ and 3′ UTRs that may be required for sgRNA transcription and genome replication. This hypothesis is also supported by deletion mutagenesis studies in which viable second-site (pseudo)revertants acquired other destabilizing mutations, most likely, to keep the stability of this structure below a certain threshold. Finally, several viable viruses were revealed to contain mutations in the 3′-UTR, providing genetic evidence for interactions between the 5′- and 3′-UTRs.

SL2 is the most conserved structure in the coronavirus 5′ UTR (Chen and Olsthoorn, 2010; Liu et al., 2007). It is comprised of a 5-bp stem and a highly conserved loop sequence, 5′-CUUGY-3′, that was shown to adopt a 5′-uYNMG(U)a- or 5′-uCUYG(U)a-like tetraloop structure (Lee et al., 2011; Liu et al., 2009). Reverse genetics data confirmed that SL2 is required for MHV replication and, possibly, sg mRNA synthesis. Within certain structural constraints, nucleotide replacements were found to be tolerated or could be rescued by increasing the stem stability, suggesting a limited plasticity of this conserved *cis*-acting RNA element (Liu et al., 2009).

3.1.2.2 Stem-Loop 3

As mentioned earlier, SL3 (named SL-II in previous BCoV DI RNA studies) appears to be conserved in a small subset of beta- and gammacoronaviruses (Chen and Olsthoorn, 2010). For BCoV and SARS-CoV, the TRS-L core sequence (CS) has been predicted to be part of this SL3 hairpin loop, a structure similar to the TRS-L hairpin structure reported for the related arterivirus equine arteritis virus (Chang et al., 1996; van den Born et al., 2004, 2005). In contrast to the situation in BCoV and SARS-CoV, the structure probing data obtained for MHV, HCoV-229E, and HCoV-NL63 suggest that the TRS-L CS and flanking regions are located in single-stranded regions (Chen and

Olsthoorn, 2010; Madhugiri et al., 2014; Stirrups et al., 2000; Wang and Zhang, 2000; Yang et al., 2015).

3.1.2.3 Stem-Loop 4

SL4 is a long hairpin structure located downstream of the TRS-L CS and has been suggested to be conserved across all coronavirus genera (Chen and Olsthoorn, 2010; Raman and Brian, 2005; Raman et al., 2003). Using a BCoV DI RNA system, a SL structure that was designated SLIII was mapped between nts 97 and 116 in the 5′-terminal genome region. The *cis*-acting function of SLIII was corroborated by studying effects of destabilizing mutations in this structural element (Raman et al., 2003). Subsequent studies by other laboratories confirmed these findings (Kang et al., 2006; Liu et al., 2007). Genus-wide bioinformatics analyses revealed that SL4 is conserved in alpha- and betacoronaviruses (Madhugiri et al., 2014). It is predicted to form a bipartite SL structure, comprised of 4a and 4b, the latter substructures being separated by a bulge (Kang et al., 2006; Liu et al., 2007; Madhugiri et al., 2014). SL4b identified by various groups corresponds to the SLIII identified by Brian and coworkers (see earlier). Furthermore, SL4 was shown to contain a short ORF comprised of just a few codons. Because of its position in the genome, upstream of the large ORF1a, it is generally referred to as the uORF. Recent reverse genetics work in the MHV system (Wu et al., 2014; Yang et al., 2011) showed that disruption of the uORF yields viable mutants that, however, evolve other uORFs upon serial passaging in cell culture. In vitro, uORF-disrupted RNAs showed enhanced translation of the downstream ORF, suggesting that the uORF represses ORF1a/1b translation and has a beneficial but nonessential role in coronavirus replication in cell culture.

Even though the 5′-terminal SL4 is conserved across the *Coronavirinae*, this hairpin structure tolerates extensive mutations. For example, it was shown for MHV that base pairing in SL4a is not required for replication and also separate deletions of SL4a and SL4b were tolerated. By contrast, deletion of the entire SL4 and a 3-nt deletion immediately downstream of SL4 abolished or profoundly impaired viral RNA synthesis. Analysis of second-site mutations and experiments using a viable MHV mutant in which SL4 was replaced with a shorter SL with a heterologous sequence led to a model in which SL4 acts as a spacer element that controls the proper orientation of SL1, SL2, and TRS-L required for subgenomic RNA synthesis (Yang et al., 2011). The SL4 sequence overlaps with the "hotspot" of the 5′-proximal genomic acceptor required for BCoV

discontinuous transcription (Wu et al., 2006), thus further supporting a role of the region immediately downstream of TRS-L in subgenomic RNA synthesis. Based on these observations, it is reasonable to think that the structural flexibility of SL4 may be required to establish transient long-range RNA–RNA interactions. In line with this idea, a previous TGEV reverse genetic study showed that mutants permitting additional base-pairing interactions of the copy TRS-B upstream of a reporter sgRNA with the 5′-GAAA-3′ sequence immediately downstream of the TGEV TRS-L CS (5′-ACUAAAC-3′) enhance the production of this particular reporter sgRNA (Zúñiga et al., 2004). Based on the available functional data and structural analyses of alphacoronavirus 5′-terminal genome regions, it was proposed that the basal part of SL4 exists in a flexible state, thereby possibly facilitating strand transfer during sg minus-strand RNA synthesis (Zúñiga et al., 2004). In addition to the inherent SL4 structural flexibility, proteins known to bind to this region may additionally modulate the stability of the SL4 structure, a hypothesis that remains to be investigated in further experiments. Of particular interest in this context, heterogeneous nuclear ribonucleoprotein (hnRNP) family members and the viral N protein have been shown to bind to this region and there is evidence that the N protein has chaperone functions and TRS-L/TRS-B unwinding activities (Galan et al., 2009; Grossoehme et al., 2009; Huang and Lai, 1999; Keane et al., 2012; Li et al., 1997, 1999; Shi and Lai, 2005; Sola et al., 2011a,b; Zúñiga et al., 2007, 2010). It is therefore tempting to speculate that cellular and/or viral proteins bind and unwind the energetically labile SL4 substructure to facilitate the strand transfer during sg minus-strand RNA synthesis.

3.1.2.4 Stem-Loop 5

A 5′-terminal SL designated earlier as SL-IV that extends into the nsp1 coding sequence was described as an RNA element required for optimal MHV replication (Guan et al., 2011). The SHAPE analysis mentioned earlier suggests that SL5 contains three hairpin substructures, SL5a (previously designated as SL-IV), 5b, and 5c (Yang et al., 2015). Genus-wide analyses of 5′-terminal genome regions suggest a similar SL5 structure to be conserved in alphacoronaviruses, which includes three substructures called SL5a, 5b, and 5c (Chen and Olsthoorn, 2010; Madhugiri et al., 2014). In both alpha- and betacoronaviruses, SL5 extends into ORF1a. Depending on the lineage studied, conserved loop sequences could be identified in the hairpin substructures of SL5. This sequence conservation was more pronounced in alpha- than in betacoronaviruses. In alphacoronaviruses,

each of the three hairpins (SL5a, 5b, and 5c) was found to contain a 5′-UUCCGU-3′ loop sequence (Madhugiri et al., 2014). Equivalent structures in betacoronaviruses were only partly conserved, with significant lineage-specific variations being detectable in the substructural hairpins and their terminal loop sequences. A possible SL5 equivalent in gammacoronaviruses was predicted to adopt a rod-like structure that lacks conserved loop sequences (Chen and Olsthoorn, 2010).

As outlined earlier, possible betacoronavirus SL5 substructures located within (or extending into) the nsp1-coding region (previously termed SLs IV, V, VI, and VII) have been characterized structurally and functionally using BCoV DI RNA and MHV reverse genetics systems (Brown et al., 2007; Guan et al., 2011, 2012; Raman and Brian, 2005). In a BCoV-based DI RNA system, SL5A (previously designated as SL-IV) was revealed to be a *cis*-acting element essential for DI RNA replication (Brown et al., 2007). In a recent MHV reverse genetic study, nucleotide substitutions that disrupt SL5C while preserving the N-terminal nsp1 amino acid sequence resulted in the recovery of viable mutant viruses with only moderate impairment of virus replication compared to wild-type virus, implying that SL5C is dispensable for viral replication (Yang et al., 2015) while earlier studies suggested this region to be required for accumulation and replication of a BCoV-based DI RNA (Brown et al., 2007). The reasons for these contradictory results are not clear but may be linked to limitations of DI-based replication assays in which even small functional defects may result in a complete loss of DI RNA replication. Similar observations were made in other cases. For example, DI RNAs and recombinant viruses containing identical mutations in the 5′- and 3′-UTRs led to quite different phenotypes in some cases (Johnson et al., 2005; Yang et al., 2011), illustrating that reverse genetics systems based on full-length genomes are powerful and, in some cases, essential tools in functional studies of *cis*-acting elements.

3.2 3′-Terminal *cis*-Acting RNA Elements

The first studies of 3′ *cis*-acting elements required for RNA replication were based on betacoronavirus DI RNA systems (Kim et al., 1993; Lin and Lai, 1993; Luytjes et al., 1996). Coronavirus 3′ UTRs range in size from ~300 to ~500 nts (excluding the 3′ poly(A) tail). Using MHV DI RNAs, the minimal length of 3′-terminal sequence required for replication was determined to involve 436 nts, including the entire 301-nt 3′ UTR, part of the N protein-coding sequence and the poly(A) tail (Lin et al., 1996; Luytjes

et al., 1996). In subsequent studies, the minimal 3′-terminal sequences required for TGEV (492 nts) and IBV (338 nts) DI RNA replication were determined (Dalton et al., 2001; Mendez et al., 1996). In both viruses, the *cis*-acting signal required for RNA synthesis could be mapped to the 3′-UTR (only), while N protein-coding sequences were not required. Similar observations were made for betacoronaviruses using recombinant MHV mutants. These studies demonstrated that the structural protein genes (including the N protein-coding region) tolerate substantial alterations including combinations of single-site mutations and rearrangements of entire genes, suggesting that the 3′-proximal coding regions are not part of the 3′ *cis*-acting elements (de Haan et al., 2002; Goebel et al., 2004b; Lorenz et al., 2011). Furthermore, studies by Enjuanes and coworkers suggested that the N gene was dispensable for replication of *Alphacoronavirus 1* using both TGEV and FCoV (Izeta et al., 1999). Also, deletions of the FCoV accessory protein genes 7a and 7b were shown to be tolerated, demonstrating that the 3′ *cis*-acting replication signals of this virus involve only 283 nts plus poly(A) tail (Haijema et al., 2004). For MHV, the minimal 3′-terminal *cis*-acting signal required for negative-strand (but not plus-strand) RNA synthesis was mapped to no more than 55 nts using a DI RNA-based system (Lin et al., 1994). Furthermore, a short poly(A) tract of at least 5–10 nts was shown to be an essential *cis*-acting signal to support BCoV DI RNA replication (Spagnolo and Hogue, 2000).

3.2.1 Structural Features of Coronavirus 3′ cis-Acting Elements

Also in this case, our knowledge of coronavirus 3′ *cis*-acting elements is largely based on studies using betacoronaviruses, such as MHV. A combination of bioinformatics, biochemical analyses, and functional studies was used to identify and characterize *cis*-acting RNA elements in the 3′ UTR (Goebel et al., 2004a, 2007; Hsue and Masters, 1997; Hsue et al., 2000; Liu et al., 2001, 2013; Stammler et al., 2011; Williams et al., 1999; Züst et al., 2008). More recently, these studies were extended to alphacoronaviruses using genus-wide bioinformatics analyses. A combination of sequence and structural alignments of all currently recognized alphacoronavirus species was used to identify conserved RNA structures in the 3′-terminal genome region and the predicted structures were then confirmed and refined using structure probing data obtained for HCoV-229E and HCoV-NL63 (Madhugiri et al., 2014). Fig. 1 provides a simplistic representation of the 3′-proximal RNA structures identified in beta- and alphacoronaviruses.

The 5′-most RNA structure in this region is a bulged stem-loop (BSL) of 68 nts. It is located immediately downstream of the N gene stop codon and was shown to be required for MHV DI RNA replication (Hsue and Masters, 1997; Hsue et al., 2000). Despite limited sequence similarity in this genome region, the BSL structure is predicted to be conserved in betacoronaviruses (Goebel et al., 2004a; Hsue and Masters, 1997). A possible BSL equivalent was also identified in IBV and other gammacoronaviruses and its functional importance was supported using IBV DI RNA constructs (Dalton et al., 2001). The nearly perfect SL structure in IBV comprises 42 nts and is located at the upstream end of region II, a conserved region in the gammacoronavirus 3′ UTR. Recent structural and bioinformatics analyses suggest that alphacoronavirus 3′ UTRs do not contain a structural equivalent of the betacoronavirus BSL (Madhugiri et al., 2014).

The second essential RNA structure positioned 3′ to the BSL is a classical hairpin-type pseudoknot (PK) structure, which was first identified in BCoV. This 54-nt RNA element was identified as a *cis*-acting element required for BCoV DI RNA replication (Williams et al., 1999). Also the 3′-terminal genome regions of other betacoronaviruses, such as HCoV-HKU1 (Woo et al., 2005) and SARS-CoV, were found to contain this PK structure (Goebel et al., 2004b). Other studies suggested that this PK structure was conserved in beta- and alphacoronaviruses while gammacoronaviruses retained only some of the PK features or lacked this structure entirely (Williams et al., 1999). An interesting structural property of the BSL and the PK is that the elements overlap by five nucleotides in the primary structure. This implies that they cannot exist simultaneously, at least not completely, which led to a model in which the BSL and PK are part of a "molecular switch" that regulates viral RNA synthesis. Evidence to support this model was obtained in an extensive MHV mutagenesis study (Goebel et al., 2004a).

A recent bioinformatics study revisited the conservation of RNA structural elements in the betacoronavirus 3′ UTR, including the BSL and the two SL structures that form the PK. The predictions were in excellent agreement with previous studies (Goebel et al., 2004a) and confirmed that, in all established betacoronavirus species, the formation of the PK requires structural rearrangements at the base of the BSL to permit the base-pairing interactions required to form PK stem 1, the latter involving the loop sequence of the PK-SL2 element and the BSL 3′-terminal sequence (Madhugiri et al., 2014). Interestingly, this study also revealed another conserved structural element, a short hairpin, immediately upstream of the PK-SL2 and suggested

that the formation of this hairpin may compete with base-pairing interactions required to form the basal part of the BSL and the PK stem 1, respectively. Furthermore, this hairpin overlaps partly with the PK loop 1 region that, in a previous study, was suggested to interact with the extreme 3′ end of the MHV genome (Züst et al., 2008). The conservation of both structure and sequence of this hairpin supports a biological function of this element. In this context, it may be worth mentioning that the hairpin structure is predicted to be disrupted by the 6-nt insertion in loop 1 that, previously, was reported to cause a poorly replicating and unstable phenotype in MHV (Goebel et al., 2004a). It remains to be seen if the small hairpin represents yet another element in the intricate network of base-pairing interactions between the BSL, the PK, and the 3′ end that together constitute the complex molecular switch proposed by the Masters laboratory (Goebel et al., 2004a).

Our recent study using representative viruses from all currently recognized alphacoronavirus species identified a number of conserved RNA structural elements in the alphacoronavirus 3′ UTR (Madhugiri et al., 2014). As described earlier, a counterpart of the betacoronavirus BSL structure (Goebel et al., 2004a; Hsue and Masters, 1997) could not be identified in the alphacoronavirus 3′ UTR, while structural elements required to form a PK structure were identified in all alphacoronaviruses (Madhugiri et al., 2014). Intriguingly, despite the absence of an upstream BSL in alphacoronaviruses, the formation of this putative PK structure was predicted to require the disruption of a short hairpin immediately upstream of PK-SL2, a scenario that is similar to (but less complex than) that described for betacoronaviruses. Further studies are required to answer the question of whether or not alphacoronaviruses employ a molecular switch mechanism similar to that employed by betacoronaviruses (Goebel et al., 2004a). Furthermore, our structure probing analyses supported the predicted PK-SL2 structure for both HCoV-229E and HCoV-NL63 (Madhugiri et al., 2014). They also supported base-pairing interactions upstream of the HCoV-NL63 SL2, thus supporting the formation of the predicted small hairpin in this region, while we failed to obtain experimental support for this hairpin in HCoV-229E. Also, the structure probing data did not support the formation of a stable PK structure, possibly reflecting a low thermodynamic stability as previously reported for the equivalent PK in betacoronaviruses (Stammler et al., 2011). Further experiments including reverse genetics studies are required to confirm the existence and biological significance of the predicted alphacoronavirus PK structure.

The 3′-most RNA secondary structure, a long multibranched SL structure downstream of the pseudoknot was predicted and further confirmed by biochemical probing (Liu et al., 2001). For MHV, several of the stems in this region were reported to be required for efficient DI RNA replication. Using an MHV reverse genetic approach, Masters and coworkers demonstrated that the long hypervariable BSL structure is dispensable for viral replication (Goebel et al., 2007). The study by Madhugiri et al. (2014) revealed the conservation of this RNA structural element downstream of PK-SL2 in all betacoronaviruses and, as expected, confirmed the conservation of the octanucleotide sequence, 5′-GGAAGAGC-3′, that has been identified previously in the 3′ UTR of most coronaviruses (Goebel et al., 2007). The octanucleotide sequence was confirmed to be part of a single-stranded region. As pointed out earlier, the role of this conserved element is currently unclear as both the HVR and the octanucleotide sequence appear to be dispensable for MHV replication in vitro (Goebel et al., 2007; Liu et al., 2001).

With respect to the HVR downstream of PK-SL2, an extensive SL structure was predicted in bioinformatics analyses of alphacoronavirus 3′ UTRs (Madhugiri et al., 2014). The structure is supported by a large number of covariant base pairs and contains the conserved octanucleotide sequence in a single-stranded region, which could be corroborated by structure probing data obtained for HCoV-229E and HCoV-NL63. Of note, the cell culture-adapted HCoV-NL63 isolate used in our study for structure probing analysis contained a short deletion (apparently acquired during serial passaging in cell culture) that resulted in a smaller loop but retained the octanucleotide sequence (with one G-to-A replacement) in a position identical to that predicted for HCoV-229E (Madhugiri et al., 2014). This serendipitous deletion shows that the distal part of the extended SL structure is dispensable for HCoV-NL63 replication in cell culture. The data also suggested that, despite the deletion, the octanucleotide sequence retains a position in the loop region of the SL structure and tolerates minimal changes, the latter being consistent with MHV reverse genetics data obtained for the HVR/octanucleotide region (Goebel et al., 2007).

3.2.2 Functional Roles of Coronavirus 3′-Terminal cis-Acting Elements

Possible functions of RNA elements residing in the 3′-proximal genome regions have been studied most extensively in betacoronaviruses. Although the betacoronavirus 3′ UTRs have minimal sequence identity, the RNA structures conserved across different betacoronavirus lineages appear to be functionally equivalent as demonstrated in studies using viable chimeric

viruses. Intriguingly, this functional conservation of 3′-proximal RNA structures does not extend to alpha- and gammacoronaviruses because replacements of the MHV 3′ UTR with that of TGEV and IBV, respectively, did not give rise to viable MHV mutants (Goebel et al., 2004b). The available evidence suggests that coronaviruses evolved several genus-specific *cis*-acting RNA elements. For example, the presence of a BSL followed by a PK structure is limited to betacoronaviruses, while other genera appear to contain only one of these elements, with the PK being conserved in alphacoronaviruses and the BSL in gammacoronaviruses (Dalton et al., 2001; Hsue and Masters, 1997; Williams et al., 1999).

3.2.2.1 BSL and Pseudoknot

The structures and several potentially important substructures of both the BSL and PK have been characterized in significant detail for BCoV and MHV (Goebel et al., 2004a; Hsue et al., 2000; Williams et al., 1999). As indicated earlier, the BSL and PK regions overlap by several nucleotides. Formation of the first stem of the PK structure requires base-pairing interactions with the downstream segment F of the BSL, thereby disrupting the basal part of this structure. In a comprehensive MHV mutagenesis study, the functional significance of both structures was demonstrated conclusively. Because the two structures cannot exist simultaneously and, yet, each of them is essential for viral replication, it was proposed that the two elements may adopt substructures that act as a "molecular switch" that controls the transition between different steps of the viral replication cycle (Goebel et al., 2004a). In a subsequent study, the proposed "molecular switch" was characterized in more detail and evidence was obtained to suggest a direct interaction between loop 1 of the PK with the extreme 3′ end of the MHV genome (Züst et al., 2008). The characterization of second-site revertants arising from MHV mutants with genetically engineered insertions in loop 1 revealed distinct replacements at the extreme 3′ end, thereby retaining specific base-pairing interactions with the loop 1 region and thus precluding the formation of stem 1 of the PK. Other mutants were found to contain second-site replacements indicative of RNA:protein interactions between the PK region and nsp8 and nsp9. Based on these data, a model was proposed in which the formation and disruption of the PK by differential base-pairing interactions with the BSL and 3′-terminal genome sequences, respectively, may lead to alternate substructures that govern different steps of the initiation and continuation of negative-strand RNA synthesis (Züst et al., 2008). Further evidence to support this model was

obtained in a subsequent MHV reverse genetics study by Liu et al. (2013). Thermodynamic investigations revealed a limited stability of the PK structure (Stammler et al., 2011). This structural flexibility is consistent with the proposed role as a "molecular switch."

3.2.2.2 Hypervariable Region

The region downstream of the PK is less conserved among betacoronaviruses. It is generally referred to as the "hypervariable region (HVR)" and is not identical to the "HVR" identified at the 5′ end of the 3′ UTR in IBV (Dalton et al., 2001; Williams et al., 1993). The betacoronavirus HVR was predicted to contain a complex and functionally relevant RNA structure based on enzymatic probing and MHV DI RNA mutagenesis data (Liu et al., 2001). By contrast, more recent studies showed that large parts or even the entire HVR region can be deleted without causing major defects in MHV replication, arguing against an essential role of this genome region in viral replication (Goebel et al., 2007; Züst et al., 2008). However, some of the MHV HVR mutants proved to be highly attenuated in vivo, suggesting a possible role in pathogenesis (Goebel et al., 2007).

The conserved octanucleotide sequence mentioned earlier, 5′-GGAAGAGC-3′, was identified in early coronavirus sequence analyses performed in the late 1980s (Boursnell et al., 1985; Lapps et al., 1987; Schreiber et al., 1989). Subsequent studies confirmed its universal conservation across all coronavirus genera, with only very few viruses containing single replacements in this sequence (Goebel et al., 2007). Obviously, this strict conservation suggests an important functional role which, however, could not be confirmed to date. As mentioned earlier, the entire HVR including the octanucleotide sequence can be deleted from the MHV genome without causing major defects in viral replication in vitro (Goebel et al., 2007). In line with this, replacements of single nucleotides within the octanucleotide motif were tolerated although most of these mutants exhibited small-plaque phenotypes and/or delayed single-step growth kinetics. In both high- and low-multiplicity-of-infection experiments, octanucleotide and HVR deletion mutants lagged behind the wild-type virus but reached near-wild-type titers at later time points and had no detectable defect in viral RNA synthesis (Goebel et al., 2007).

3.2.2.3 3′-Terminal Poly(A) Tail

MHV and BCoV DI RNA studies showed that the poly(A) tail at the 3′ end of coronavirus genomes is essential, with a minimum of 5–10 adenylate

residues being required for DI RNA replication (Spagnolo and Hogue, 2000). This requirement corresponds well to the minimal binding site of the poly(A)-binding protein (PABP) on DI RNAs poly(A) sequences (Spagnolo and Hogue, 2000). Recent studies further suggest that 3′ poly(A) tail lengths may vary between 30 and 65 nt in the course of viral replication in vitro (Wu et al., 2013) as was shown for both beta- and gammacoronavirus infections and in a range of cell types, both in vitro and in vivo (Shien et al., 2014). The biological significance of these observations is currently unclear.

4. RNA ELEMENTS INVOLVED IN CORONAVIRUS GENOME PACKAGING

To selectively package their genome RNA (rather than other viral and cellular RNAs), viruses employ distinct *cis*-acting sequences in the viral genome RNA and *trans*-acting viral factors (Annamalai and Rao, 2006; D'Souza and Summers, 2005; Nugent et al., 1999). Even though coronaviruses produce large amounts of subgenomic mRNAs in infected cells, these RNAs are not (or extremely inefficiently) incorporated into virus particles (Escors et al., 2003), suggesting that coronaviruses have evolved specific mechanisms to efficiently package their genome RNA into progeny virus particles.

Like for other coronavirus *cis*-acting RNA elements, the genomic packaging signal (PS) was first discovered by DI RNA studies using MHV (Makino et al., 1990; van der Most et al., 1991). PSs of alpha- and gammacoronaviruses were first identified for TGEV and IBV (Escors et al., 2003; Penzes et al., 1994). MHV DI RNA studies revealed a 69-nt SL structure that was (i) located in the 3′ region of ORF1b, (ii) confirmed to be required for DI RNA packaging, and (iii) shown to interact with the viral N protein (Fosmire et al., 1992; Molenkamp and Spaan, 1997; Woo et al., 1997). Subsequent studies indicated that a larger PS element and, possibly, additional factors are required for optimal packaging efficiency (Bos et al., 1997; Cologna and Hogue, 2000; Narayanan and Makino, 2001). More recently, a PS that is conserved in lineage A betacoronaviruses and a novel 95-nt BSL were predicted and supported by chemical and enzymatic probing experiments (Chen et al., 2007). The conservation of this PS among lineage A coronaviruses is consistent with earlier observations that the BCoV PS is functionally replaceable with its MHV counterpart (Cologna and Hogue, 2000). Remarkably, this

structurally and functionally conserved PS of lineage A betacoronaviruses is not conserved in other lineages of betacoronaviruses and other coronavirus genera (Kuo and Masters, 2013), suggesting differential requirements for genome packaging among closely related coronaviruses.

For TGEV, the PS was identified using genetically engineered DI RNAs (Izeta et al., 1999). Deletion analyses revealed a minimal TGEV PS required for efficient packaging. This PS contained nts 100–649 from the 5′-proximal genome region (Escors et al., 2003). Also for IBV, a DI RNA that was efficiently packaged has been isolated and characterized (Penzes et al., 1994), even though, in this case, the mapping of a possible PS produced inconclusive data (Dalton et al., 2001). The TGEV and IBV studies support the notion above that coronavirus PSs are found in different genome regions (Escors et al., 2003; Penzes et al., 1994) which, to some extent, is reminiscent of the situation described for picornavirus *cre* elements (Steil and Barton, 2009).

Further insight into the role of PS in genome RNA packaging into virions was obtained in a recent study using MHV (Kuo and Masters, 2013). The study provides conclusive evidence that (i) the PS supports selective packaging of the viral genome RNA into virions and (ii) remains functional when transposed to an ectopic genomic site. Surprisingly, this study also revealed that the PS is not essential for MHV viability and viral growth in cell culture, suggesting that the principal role of the MHV PS is to ensure selective packaging of viral genome RNA into virions. Further insight into conserved and distinct properties of coronaviruses PSs can be expected from future studies using viruses representing all established coronavirus genera.

5. POSSIBLE ROLES OF CELLULAR PROTEINS IN CORONAVIRUS REPLICATION

A number of studies have addressed possible roles of cellular proteins in coronavirus (mainly MHV) RNA synthesis. In these studies, several members of the hnRNP family (PTB or hnRNP A1, SYNCRIP) were identified based on their ability to bind to viral RNA fragments containing TRS (TRS-L as well as TRS-B) in vitro and, in some cases, to affect MHV replication (Choi et al., 2004; Furuya and Lai, 1993; Li et al., 1997; Zhang and Lai, 1995). Deletion analysis and site-directed mutagenesis of the binding regions of PTB or hnRNP A1 further demonstrated significant inhibition of RNA transcription (Li et al., 1999). Furthermore, the functional importance of hnRNP in coronavirus RNA

replication was demonstrated by overexpressing wild-type hnRNP A1 or a dominant-negative form of hnRNP A1 in cells (Shi et al., 2000, 2003). It was also shown that hnRNP A1 interacts with the viral N protein (both in vitro and in vivo), suggesting that this protein may become part of the RTC (Shi et al., 2000; Wang and Zhang, 1999). Members of the hnRNP family (hnRNP A1 and PTB) were shown to bind to 5′ UTR and 3′ UTR and were suggested to mediate a cross talk between 5′- and 3′-terminal genome regions (Huang and Lai, 1999, 2001). Furthermore, it was reported that interactions of hnRNP A1 and PTB modulate viral RNA synthesis and SYNCRIP silencing leads to reduced virus production (Choi et al., 2004). Similar observations were made for TGEV. It was shown that PTB binds to the TGEV TRS-L sequence while other hnRNP family members were found to bind to the 3′ end of the genome (hnRNP Q, hnRNP A2B1, and hnRNP A0) (Galan et al., 2009; Sola et al., 2011b). Furthermore, silencing of hnRNP Q expression showed a significant reduction in TGEV RNA synthesis and virus production, supporting biologically relevant functions of hnRNP family members in coronavirus RNA synthesis (Galan et al., 2009). Host factors that interact with specific 5′ *cis*-acting structures have only been described for BCoV (Raman and Brian, 2005). These host factors were revealed to bind to SL 5a (previously designated as SL-IV).

Proteins that specifically interact with coronavirus 3′ UTRs have mainly been identified by UV-crosslinking experiments using MHV, BCoV, and TGEV terminal genome sequences (Sola et al., 2011b). Members of the hnRNP family and several other proteins were shown to interact with the 3′ UTR and have been suggested to have a role in negative-strand as well as positive-strand (genomic and subgenomic) RNA synthesis (Sola et al., 2011b). For BCoV, immunoprecipitation experiments revealed several proteins, including PABP, to interact with the poly(A) tail, another important *cis*-acting element for coronavirus replication (Spagnolo and Hogue, 2000). As mentioned earlier, several proteins, including PABP, could be enriched by RNA affinity chromatography using the TGEV 3′ UTR (Galan et al., 2009). Silencing of PABP, hnRNP Q, and glutamyl-prolyl-tRNA synthetase expression led to a two- to threefold reduction in viral RNA synthesis, suggesting that host factors that specifically interact with viral *cis*-acting elements may affect (or even be essential for) viral RNA replication. Clearly, the possible functions of these cellular factors deserve further investigation.

In addition to their interactions with *cis*-acting RNA elements, cellular proteins were found to interact with specific coronavirus nsps. For example, the purification and characterization of enzymatically active SARS-CoV RTCs showed that cellular factors may enhance viral RdRp activity (van Hemert et al., 2008). Also, cellular DEAD-box-family helicases, such as DDX5 and DDX1, have been implicated in coronavirus RNA synthesis. Specific interactions of the DDX5 protein with the SARS-CoV helicase, nsp13, were confirmed in yeast and mammalian two-hybrid and co-immunoprecipitation experiments. Silencing of DDX5 expression led to reduced viral RNA replication and virus titers, supporting the biological significance of this interaction (Chen et al., 2009a). Similarly, in IBV and SARS-CoV, interactions between DDX1 and nsp14 were identified by yeast two-hybrid and coimmunoprecipitation assays (Xu et al., 2010) and validated by showing that knockdown of DDX1 expression affects coronavirus RNA replication and transcription. Similar conclusions were drawn from TGEV TRS interaction studies. Also in this context, the DDX1 helicase was suggested to have a role in coronavirus replication (Sola et al., 2011b).

6. CONCLUSIONS AND OUTLOOK

Over the past years, a large number of studies using structural, biochemical, and reverse genetics approaches have provided important new insight into *cis*-acting elements that drive and control coronavirus RNA replication (reviewed in Masters, 2007; Sola et al., 2011b). In many cases, these studies used betacoronaviruses, while alpha- and gammacoronaviruses were studied to a lesser extent and there is essentially no information on deltacoronaviruses. This work also identified a growing number of cellular and viral proteins that bind to these structures and may have functions in genomic and/or subgenomic RNA synthesis, genome packaging, genome expression, or intracellular targeting of factors/structures engaged in viral RNA synthesis (reviewed in Narayanan and Makino, 2007; Sola et al., 2011b).

Recent bioinformatic studies suggest that the RNA secondary structure elements identified to date for only a small number of coronaviruses may be significantly more conserved than previously thought, both within and across the four coronavirus genera (Chen and Olsthoorn, 2010; Madhugiri et al., 2014; Yang et al., 2015). These studies also provide

evidence to suggest a coevolution of RNA structures in the terminal genome regions with the viral replication machinery. Consistent with this hypothesis, the level of conservation of 5′- and 3′-terminal *cis*-active RNA elements among different coronavirus genera and lineages was found to be largely consistent with the replicase gene-based classification of the *Coronavirinae* (de Groot et al., 2012a; Madhugiri et al., 2014). The most conserved elements identified to date include SL 1, 2, and 4 (possibly, also SL 5) in the 5′ genome region and a putative PK in the 3′-UTR. The precise roles of these structures and the viral and cellular proteins that bind these structures to perform specific steps in viral RNA synthesis remain to be investigated in more detail. Another interesting aspect to be explored in future studies should address a possible role of the coronavirus 3′-UTR in specific virus–host interactions and/or pathogenesis (Goebel et al., 2007).

ACKNOWLEDGMENTS

The work of R.M. and J.Z. is supported by grants from the Deutsche Forschungsgemeinschaft (SFB 1021, A01, and B01).

REFERENCES

Almazan, F., Gonzalez, J.M., Penzes, Z., Izeta, A., Calvo, E., Plana-Duran, J., et al., 2000. Engineering the largest RNA virus genome as an infectious bacterial artificial chromosome. Proc. Natl. Acad. Sci. U.S.A. 97, 5516–5521.

Almazan, F., Galan, C., Enjuanes, L., 2004. The nucleoprotein is required for efficient coronavirus genome replication. J. Virol. 78, 12683–12688.

Anand, K., Palm, G.J., Mesters, J.R., Siddell, S.G., Ziebuhr, J., Hilgenfeld, R., 2002. Structure of coronavirus main proteinase reveals combination of a chymotrypsin fold with an extra alpha-helical domain. EMBO J. 21, 3213–3224.

Anand, K., Ziebuhr, J., Wadhwani, P., Mesters, J.R., Hilgenfeld, R., 2003. Coronavirus main proteinase (3CLpro) structure: basis for design of anti-SARS drugs. Science 300, 1763–1767.

Annamalai, P., Rao, A.L., 2006. Packaging of brome mosaic virus subgenomic RNA is functionally coupled to replication-dependent transcription and translation of coat protein. J. Virol. 80, 10096–10108.

Baker, S.C., Shieh, C.K., Soe, L.H., Chang, M.F., Vannier, D.M., Lai, M.M., 1989. Identification of a domain required for autoproteolytic cleavage of murine coronavirus gene A polyprotein. J. Virol. 63, 3693–3699.

Bos, E.C., Dobbe, J.C., Luytjes, W., Spaan, W.J., 1997. A subgenomic mRNA transcript of the coronavirus mouse hepatitis virus strain A59 defective interfering (DI) RNA is packaged when it contains the DI packaging signal. J. Virol. 71, 5684–5687.

Boursnell, M.E., Binns, M.M., Foulds, I.J., Brown, T.D., 1985. Sequences of the nucleocapsid genes from two strains of avian infectious bronchitis virus. J. Gen. Virol. 66, 573–580.

Boursnell, M.E., Brown, T.D., Foulds, I.J., Green, P.F., Tomley, F.M., Binns, M.M., 1987. Completion of the sequence of the genome of the coronavirus avian infectious bronchitis virus. J. Gen. Virol. 68, 57–77.

Bouvet, M., Lugari, A., Posthuma, C.C., Zevenhoven, J.C., Bernard, S., Betzi, S., et al., 2014. Coronavirus Nsp10: a critical co-factor for activation of multiple replicative enzymes. J. Biol. Chem. 289, 25783–25796.

Brian, D.A., Baric, R.S., 2005. Coronavirus genome structure and replication. Curr. Top. Microbiol. Immunol. 287, 1–30.

Brian, D.A., Spaan, W.J.M., 1997. Recombination and coronavirus defective interfering RNAs. Semin. Virol. 8, 101–111.

Brierley, I., Boursnell, M.E., Binns, M.M., Bilimoria, B., Blok, V.C., Brown, T.D., et al., 1987. An efficient ribosomal frame-shifting signal in the polymerase-encoding region of the coronavirus IBV. EMBO J. 6, 3779–3785.

Brierley, I., Digard, P., Inglis, S.C., 1989. Characterization of an efficient coronavirus ribosomal frameshifting signal: requirement for an RNA pseudoknot. Cell 57, 537–547.

Brockway, S.M., Denison, M.R., 2005. Mutagenesis of the murine hepatitis virus nsp1-coding region identifies residues important for protein processing, viral RNA synthesis, and viral replication. Virology 340, 209–223.

Brown, C.G., Nixon, K.S., Senanayake, S.D., Brian, D.A., 2007. An RNA stem-loop within the bovine coronavirus nsp1 coding region is a cis-acting element in defective interfering RNA replication. J. Virol. 81, 7716–7724.

Casais, R., Thiel, V., Siddell, S.G., Cavanagh, D., Britton, P., 2001. Reverse genetics system for the avian coronavirus infectious bronchitis virus. J. Virol. 75, 12359–12369.

Chang, R.Y., Hofmann, M.A., Sethna, P.B., Brian, D.A., 1994. A cis-acting function for the coronavirus leader in defective interfering RNA replication. J. Virol. 68, 8223–8231.

Chang, R.Y., Krishnan, R., Brian, D.A., 1996. The UCUAAAC promoter motif is not required for high-frequency leader recombination in bovine coronavirus defective interfering RNA. J. Virol. 70, 2720–2729.

Chen, S.C., Olsthoorn, R.C., 2010. Group-specific structural features of the 5′-proximal sequences of coronavirus genomic RNAs. Virology 401, 29–41.

Chen, S.C., van den Born, E., van den Worm, S.H., Pleij, C.W., Snijder, E.J., Olsthoorn, R.C., 2007. New structure model for the packaging signal in the genome of group IIa coronaviruses. J. Virol. 81, 6771–6774.

Chen, J.Y., Chen, W.N., Poon, K.M., Zheng, B.J., Lin, X., Wang, Y.X., et al., 2009a. Interaction between SARS-CoV helicase and a multifunctional cellular protein (Ddx5) revealed by yeast and mammalian cell two-hybrid systems. Arch. Virol. 154, 507–512.

Chen, Y., Cai, H., Pan, J., Xiang, N., Tien, P., Ahola, T., et al., 2009b. Functional screen reveals SARS coronavirus nonstructural protein nsp14 as a novel cap N7 methyltransferase. Proc. Natl. Acad. Sci. U.S.A. 106, 3484–3489.

Chen, Y., Su, C., Ke, M., Jin, X., Xu, L., Zhang, Z., et al., 2011. Biochemical and structural insights into the mechanisms of SARS coronavirus RNA ribose 2′-O-methylation by nsp16/nsp10 protein complex. PLoS Pathog. 7, e1002294.

Choi, K.S., Mizutani, A., Lai, M.M., 2004. SYNCRIP, a member of the heterogeneous nuclear ribonucleoprotein family, is involved in mouse hepatitis virus RNA synthesis. J. Virol. 78, 13153–13162.

Cologna, R., Hogue, B.G., 2000. Identification of a bovine coronavirus packaging signal. J. Virol. 74, 580–583.

Dalton, K., Casais, R., Shaw, K., Stirrups, K., Evans, S., Britton, P., et al., 2001. cis-acting sequences required for coronavirus infectious bronchitis virus defective-RNA replication and packaging. J. Virol. 75, 125–133.

de Groot, R.J., van der Most, R.G., Spaan, W.J., 1992. The fitness of defective interfering murine coronavirus DI-a and its derivatives is decreased by nonsense and frameshift mutations. J. Virol. 66, 5898–5905.
de Groot, R.J., Baker, S.C., Baric, R., Enjuanes, L., Gorbalenya, A.E., Holmes, K.V., et al., 2012a. Family Coronaviridae. In: King, A.M.Q., Adams, M.J., Carstens, E.B., Lefkowitz, E.J. (Eds.), Virus Taxonomy. Elsevier, Amsterdam, pp. 806–828.
de Groot, R.J., Cowley, J.A., Enjuanes, L., Faaberg, K.S., Perlman, S., Rottier, P.J.M., et al., 2012b. Order Nidovirales. In: King, A.M.Q., Adams, M.J., Carstens, E.B., Lefkowitz, E.J. (Eds.), Virus Taxonomy. Elsevier, Amsterdam, pp. 785–795.
de Haan, C.A., Volders, H., Koetzner, C.A., Masters, P.S., Rottier, P.J., 2002. Coronaviruses maintain viability despite dramatic rearrangements of the strictly conserved genome organization. J. Virol. 76, 12491–12502.
Decroly, E., Imbert, I., Coutard, B., Bouvet, M., Selisko, B., Alvarez, K., et al., 2008. Coronavirus nonstructural protein 16 is a cap-0 binding enzyme possessing (nucleoside-2′O)-methyltransferase activity. J. Virol. 82, 8071–8084.
Decroly, E., Debarnot, C., Ferron, F., Bouvet, M., Coutard, B., Imbert, I., et al., 2011. Crystal structure and functional analysis of the SARS-coronavirus RNA cap 2′-O-methyltransferase nsp10/nsp16 complex. PLoS Pathog. 7, e1002059.
den Boon, J.A., Ahlquist, P., 2010. Organelle-like membrane compartmentalization of positive-strand RNA virus replication factories. Annu. Rev. Microbiol. 64, 241–256.
Drosten, C., Günther, S., Preiser, W., van der Werf, S., Brodt, H.R., Becker, S., et al., 2003. Identification of a novel coronavirus in patients with severe acute respiratory syndrome. N. Engl. J. Med. 348, 1967–1976.
D'Souza, V., Summers, M.F., 2005. How retroviruses select their genomes. Nat. Rev. Microbiol. 3, 643–655.
Eckerle, L.D., Becker, M.M., Halpin, R.A., Li, K., Venter, E., Lu, X., et al., 2010. Infidelity of SARS-CoV Nsp14-exonuclease mutant virus replication is revealed by complete genome sequencing. PLoS Pathog. 6, e1000896.
Ehresmann, C., Baudin, F., Mougel, M., Romby, P., Ebel, J.P., Ehresmann, B., 1987. Probing the structure of RNAs in solution. Nucleic Acids Res. 15, 9109–9128.
Escors, D., Izeta, A., Capiscol, C., Enjuanes, L., 2003. Transmissible gastroenteritis coronavirus packaging signal is located at the 5′ end of the virus genome. J. Virol. 77, 7890–7902.
Fehr, A.R., Perlman, S., 2015. Coronaviruses: an overview of their replication and pathogenesis. Methods Mol. Biol. 1282, 1–23.
Fosmire, J.A., Hwang, K., Makino, S., 1992. Identification and characterization of a coronavirus packaging signal. J. Virol. 66, 3522–3530.
Furuya, T., Lai, M.M., 1993. Three different cellular proteins bind to complementary sites on the 5′-end-positive and 3′-end-negative strands of mouse hepatitis virus RNA. J. Virol. 67, 7215–7222.
Galan, C., Sola, I., Nogales, A., Thomas, B., Akoulitchev, A., Enjuanes, L., et al., 2009. Host cell proteins interacting with the 3′ end of TGEV coronavirus genome influence virus replication. Virology 391, 304–314.
Goebel, S.J., Hsue, B., Dombrowski, T.F., Masters, P.S., 2004a. Characterization of the RNA components of a putative molecular switch in the 3′ untranslated region of the murine coronavirus genome. J. Virol. 78, 669–682.
Goebel, S.J., Taylor, J., Masters, P.S., 2004b. The 3′ cis-acting genomic replication element of the severe acute respiratory syndrome coronavirus can function in the murine coronavirus genome. J. Virol. 78, 7846–7851.
Goebel, S.J., Miller, T.B., Bennett, C.J., Bernard, K.A., Masters, P.S., 2007. A hypervariable region within the 3′ cis-acting element of the murine coronavirus genome is nonessential for RNA synthesis but affects pathogenesis. J. Virol. 81, 1274–1287.

Gosert, R., Kanjanahaluethai, A., Egger, D., Bienz, K., Baker, S.C., 2002. RNA replication of mouse hepatitis virus takes place at double-membrane vesicles. J. Virol. 76, 3697–3708.

Grossoehme, N.E., Li, L., Keane, S.C., Liu, P., Dann 3rd, C.E., Leibowitz, J.L., et al., 2009. Coronavirus N protein N-terminal domain (NTD) specifically binds the transcriptional regulatory sequence (TRS) and melts TRS-cTRS RNA duplexes. J. Mol. Biol. 394, 544–557.

Guan, B.J., Wu, H.Y., Brian, D.A., 2011. An optimal cis-replication stem-loop IV in the 5′ untranslated region of the mouse coronavirus genome extends 16 nucleotides into open reading frame 1. J. Virol. 85, 5593–5605.

Guan, B.J., Su, Y.P., Wu, H.Y., Brian, D.A., 2012. Genetic evidence of a long-range RNA-RNA interaction between the genomic 5′ untranslated region and the nonstructural protein 1 coding region in murine and bovine coronaviruses. J. Virol. 86, 4631–4643.

Gustin, K.M., Guan, B.J., Dziduszko, A., Brian, D.A., 2009. Bovine coronavirus nonstructural protein 1 (p28) is an RNA binding protein that binds terminal genomic cis-replication elements. J. Virol. 83, 6087–6097.

Haijema, B.J., Volders, H., Rottier, P.J., 2004. Live, attenuated coronavirus vaccines through the directed deletion of group-specific genes provide protection against feline infectious peritonitis. J. Virol. 78, 3863–3871.

Hofmann, M.A., Brian, D.A., 1991. The 5′ end of coronavirus minus-strand RNAs contains a short poly(U) tract. J. Virol. 65, 6331–6333.

Hofmann, M.A., Sethna, P.B., Brian, D.A., 1990. Bovine coronavirus mRNA replication continues throughout persistent infection in cell culture. J. Virol. 64, 4108–4114.

Hsue, B., Masters, P.S., 1997. A bulged stem-loop structure in the 3′ untranslated region of the genome of the coronavirus mouse hepatitis virus is essential for replication. J. Virol. 71, 7567–7578.

Hsue, B., Hartshorne, T., Masters, P.S., 2000. Characterization of an essential RNA secondary structure in the 3′ untranslated region of the murine coronavirus genome. J. Virol. 74, 6911–6921.

Huang, P., Lai, M.M., 1999. Polypyrimidine tract-binding protein binds to the complementary strand of the mouse hepatitis virus 3′ untranslated region, thereby altering RNA conformation. J. Virol. 73, 9110–9116.

Huang, P., Lai, M.M., 2001. Heterogeneous nuclear ribonucleoprotein a1 binds to the 3′-untranslated region and mediates potential 5′-3′-end cross talks of mouse hepatitis virus RNA. J. Virol. 75, 5009–5017.

Huang, C., Lokugamage, K.G., Rozovics, J.M., Narayanan, K., Semler, B.L., Makino, S., 2011a. Alphacoronavirus transmissible gastroenteritis virus nsp1 protein suppresses protein translation in mammalian cells and in cell-free HeLa cell extracts but not in rabbit reticulocyte lysate. J. Virol. 85, 638–643.

Huang, C., Lokugamage, K.G., Rozovics, J.M., Narayanan, K., Semler, B.L., Makino, S., 2011b. SARS coronavirus nsp1 protein induces template-dependent endonucleolytic cleavage of mRNAs: viral mRNAs are resistant to nsp1-induced RNA cleavage. PLoS Pathog. 7, e1002433.

Imbert, I., Ulferts, R., Ziebuhr, J., Canard, B., 2010. SARS coronavirus replicative enzymes: structures and mechanisms. In: Lal, S.K. (Ed.), Molecular Biology of the SARS-Coronavirus. Springer, Berlin and Heidelberg, pp. 99–114.

Ivanov, K.A., Hertzig, T., Rozanov, M., Bayer, S., Thiel, V., Gorbalenya, A.E., et al., 2004. Major genetic marker of nidoviruses encodes a replicative endoribonuclease. Proc. Natl. Acad. Sci. U.S.A. 101, 12694–12699.

Izeta, A., Smerdou, C., Alonso, S., Penzes, Z., Mendez, A., Plana-Duran, J., et al., 1999. Replication and packaging of transmissible gastroenteritis coronavirus-derived synthetic minigenomes. J. Virol. 73, 1535–1545.

Johnson, R.F., Feng, M., Liu, P., Millership, J.J., Yount, B., Baric, R.S., et al., 2005. Effect of mutations in the mouse hepatitis virus 3′(+)42 protein binding element on RNA replication. J. Virol. 79, 14570–14585.
Kamitani, W., Narayanan, K., Huang, C., Lokugamage, K., Ikegami, T., Ito, N., et al., 2006. Severe acute respiratory syndrome coronavirus nsp1 protein suppresses host gene expression by promoting host mRNA degradation. Proc. Natl. Acad. Sci. U.S.A. 103, 12885–12890.
Kamitani, W., Huang, C., Narayanan, K., Lokugamage, K.G., Makino, S., 2009. A two-pronged strategy to suppress host protein synthesis by SARS coronavirus Nsp1 protein. Nat. Struct. Mol. Biol. 16, 1134–1140.
Kang, H., Feng, M., Schroeder, M.E., Giedroc, D.P., Leibowitz, J.L., 2006. Putative cis-acting stem-loops in the 5′ untranslated region of the severe acute respiratory syndrome coronavirus can substitute for their mouse hepatitis virus counterparts. J. Virol. 80, 10600–10614.
Kanjanahaluethai, A., Chen, Z., Jukneliene, D., Baker, S.C., 2007. Membrane topology of murine coronavirus replicase nonstructural protein 3. Virology 361, 391–401.
Keane, S.C., Liu, P., Leibowitz, J.L., Giedroc, D.P., 2012. Functional transcriptional regulatory sequence (TRS) RNA binding and helix destabilizing determinants of murine hepatitis virus (MHV) nucleocapsid (N) protein. J. Biol. Chem. 287, 7063–7073.
Kim, Y.N., Jeong, Y.S., Makino, S., 1993. Analysis of cis-acting sequences essential for coronavirus defective interfering RNA replication. Virology 197, 53–63.
Knoops, K., Kikkert, M., Worm, S.H., Zevenhoven-Dobbe, J.C., van der Meer, Y., Koster, A.J., et al., 2008. SARS-coronavirus replication is supported by a reticulovesicular network of modified endoplasmic reticulum. PLoS Biol. 6, e226.
Ksiazek, T.G., Erdman, D., Goldsmith, C.S., Zaki, S.R., Peret, T., Emery, S., et al., 2003. A novel coronavirus associated with severe acute respiratory syndrome. N. Engl. J. Med. 348, 1953–1966.
Kuo, L., Masters, P.S., 2013. Functional analysis of the murine coronavirus genomic RNA packaging signal. J. Virol. 87, 5182–5192.
Lai, M.M., Patton, C.D., Baric, R.S., Stohlman, S.A., 1983. Presence of leader sequences in the mRNA of mouse hepatitis virus. J. Virol. 46, 1027–1033.
Lapps, W., Hogue, B.G., Brian, D.A., 1987. Sequence analysis of the bovine coronavirus nucleocapsid and matrix protein genes. Virology 157, 47–57.
Lee, C.W., Li, L., Giedroc, D.P., 2011. The solution structure of coronaviral stem-loop 2 (SL2) reveals a canonical CUYG tetraloop fold. FEBS Lett. 585, 1049–1053.
Lei, L., Ying, S., Baojun, L., Yi, Y., Xiang, H., Wenli, S., et al., 2013. Attenuation of mouse hepatitis virus by deletion of the LLRKxGxKG region of Nsp1. PLoS One 8, e61166.
Levis, R., Weiss, B.G., Tsiang, M., Huang, H., Schlesinger, S., 1986. Deletion mapping of Sindbis virus DI RNAs derived from cDNAs defines the sequences essential for replication and packaging. Cell 44, 137–145.
Li, H.P., Zhang, X., Duncan, R., Comai, L., Lai, M.M., 1997. Heterogeneous nuclear ribonucleoprotein A1 binds to the transcription-regulatory region of mouse hepatitis virus RNA. Proc. Natl. Acad. Sci. U.S.A. 94, 9544–9549.
Li, H.P., Huang, P., Park, S., Lai, M.M., 1999. Polypyrimidine tract-binding protein binds to the leader RNA of mouse hepatitis virus and serves as a regulator of viral transcription. J. Virol. 73, 772–777.
Li, L., Kang, H., Liu, P., Makkinje, N., Williamson, S.T., Leibowitz, J.L., et al., 2008. Structural lability in stem-loop 1 drives a 5′ UTR-3′ UTR interaction in coronavirus replication. J. Mol. Biol. 377, 790–803.
Liao, C.L., Lai, M.M., 1994. Requirement of the 5′-end genomic sequence as an upstream cis-acting element for coronavirus subgenomic mRNA transcription. J. Virol. 68, 4727–4737.

Lin, Y.J., Lai, M.M., 1993. Deletion mapping of a mouse hepatitis virus defective interfering RNA reveals the requirement of an internal and discontiguous sequence for replication. J. Virol. 67, 6110–6118.
Lin, Y.J., Liao, C.L., Lai, M.M., 1994. Identification of the cis-acting signal for minus-strand RNA synthesis of a murine coronavirus: implications for the role of minus-strand RNA in RNA replication and transcription. J. Virol. 68, 8131–8140.
Lin, Y.J., Zhang, X., Wu, R.C., Lai, M.M., 1996. The 3′ untranslated region of coronavirus RNA is required for subgenomic mRNA transcription from a defective interfering RNA. J. Virol. 70, 7236–7240.
Liu, Q., Johnson, R.F., Leibowitz, J.L., 2001. Secondary structural elements within the 3′ untranslated region of mouse hepatitis virus strain JHM genomic RNA. J. Virol. 75, 12105–12113.
Liu, P., Li, L., Millership, J.J., Kang, H., Leibowitz, J.L., Giedroc, D.P., 2007. A U-turn motif-containing stem-loop in the coronavirus 5′ untranslated region plays a functional role in replication. RNA 13, 763–780.
Liu, P., Li, L., Keane, S.C., Yang, D., Leibowitz, J.L., Giedroc, D.P., 2009. Mouse hepatitis virus stem-loop 2 adopts a uYNMG(U)a-like tetraloop structure that is highly functionally tolerant of base substitutions. J. Virol. 83, 12084–12093.
Liu, P., Yang, D., Carter, K., Masud, F., Leibowitz, J.L., 2013. Functional analysis of the stem loop S3 and S4 structures in the coronavirus 3′UTR. Virology 443, 40–47.
Liu, D.X., Fung, T.S., Chong, K.K., Shukla, A., Hilgenfeld, R., 2014. Accessory proteins of SARS-CoV and other coronaviruses. Antiviral Res. 109, 97–109.
Lokugamage, K.G., Narayanan, K., Huang, C., Makino, S., 2012. Severe acute respiratory syndrome coronavirus protein nsp1 is a novel eukaryotic translation inhibitor that represses multiple steps of translation initiation. J. Virol. 86, 13598–13608.
Lorenz, R., Bernhart, S.H., Honer Zu Siederdissen, C., Tafer, H., Flamm, C., Stadler, P.F., et al., 2011. ViennaRNA package 2.0. Algorithms Mol. Biol. 6, 26.
Luytjes, W., Gerritsma, H., Spaan, W.J., 1996. Replication of synthetic defective interfering RNAs derived from coronavirus mouse hepatitis virus-A59. Virology 216, 174–183.
Ma, Y., Wu, L., Shaw, N., Gao, Y., Wang, J., Sun, Y., et al., 2015. Structural basis and functional analysis of the SARS coronavirus nsp14-nsp10 complex. Proc. Natl. Acad. Sci. U.S.A. 112, 9436–9441.
Madhugiri, R., Fricke, M., Marz, M., Ziebuhr, J., 2014. RNA structure analysis of alphacoronavirus terminal genome regions. Virus Res. 194, 76–89.
Makino, S., Lai, M.M., 1990. Studies of coronavirus DI RNA replication using in vitro constructed DI cDNA clones. Adv. Exp. Med. Biol. 276, 341–347.
Makino, S., Taguchi, F., Fujiwara, K., 1984. Defective interfering particles of mouse hepatitis virus. Virology 133, 9–17.
Makino, S., Fujioka, N., Fujiwara, K., 1985. Structure of the intracellular defective viral RNAs of defective interfering particles of mouse hepatitis virus. J. Virol. 54, 329–336.
Makino, S., Shieh, C.K., Keck, J.G., Lai, M.M., 1988a. Defective-interfering particles of murine coronavirus: mechanism of synthesis of defective viral RNAs. Virology 163, 104–111.
Makino, S., Shieh, C.K., Soe, L.H., Baker, S.C., Lai, M.M., 1988b. Primary structure and translation of a defective interfering RNA of murine coronavirus. Virology 166, 550–560.
Makino, S., Yokomori, K., Lai, M.M., 1990. Analysis of efficiently packaged defective interfering RNAs of murine coronavirus: localization of a possible RNA-packaging signal. J. Virol. 64, 6045–6053.
Masters, P.S., 2006. The molecular biology of coronaviruses. Adv. Virus Res. 66, 193–292.

Masters, P.S., 2007. Genomic cis-acting elements in coronavirus RNA replication. In: Thiel, V. (Ed.), Coronaviruses—Molecular and Cellular Biology. Caister Academic Press, Norfolk, UK, pp. 65–80.
Masters, P.S., Perlman, S., 2013. Coronaviridae. In: Knipe, D.M., Howley, P.M. (Eds.), sixth ed. Fields Virology, vol. 1. Lippincott Williams & Wilkins, Philadelphia, PA, pp. 825–858.
Mendez, A., Smerdou, C., Izeta, A., Gebauer, F., Enjuanes, L., 1996. Molecular characterization of transmissible gastroenteritis coronavirus defective interfering genomes: packaging and heterogeneity. Virology 217, 495–507.
Mielech, A.M., Chen, Y., Mesecar, A.D., Baker, S.C., 2014. Nidovirus papain-like proteases: multifunctional enzymes with protease, deubiquitinating and deISGylating activities. Virus Res. 194, 184–190.
Minskaia, E., Hertzig, T., Gorbalenya, A.E., Campanacci, V., Cambillau, C., Canard, B., et al., 2006. Discovery of an RNA virus 3′→5′ exoribonuclease that is critically involved in coronavirus RNA synthesis. Proc. Natl. Acad. Sci. U.S.A. 103, 5108–5113.
Molenkamp, R., Spaan, W.J., 1997. Identification of a specific interaction between the coronavirus mouse hepatitis virus A59 nucleocapsid protein and packaging signal. Virology 239, 78–86.
Morales, L., Mateos-Gomez, P.A., Capiscol, C., del Palacio, L., Enjuanes, L., Sola, I., 2013. Transmissible gastroenteritis coronavirus genome packaging signal is located at the 5′ end of the genome and promotes viral RNA incorporation into virions in a replication-independent process. J. Virol. 87, 11579–11590.
Namy, O., Moran, S.J., Stuart, D.I., Gilbert, R.J., Brierley, I., 2006. A mechanical explanation of RNA pseudoknot function in programmed ribosomal frameshifting. Nature 441, 244–247.
Narayanan, K., Makino, S., 2001. Cooperation of an RNA packaging signal and a viral envelope protein in coronavirus RNA packaging. J. Virol. 75, 9059–9067.
Narayanan, K., Makino, S., 2007. Coronavirus genome packaging. In: Thiel, V. (Ed.), Coronaviruses—Molecular and Cellular Biology. Caister Academic Press, Norfolk, UK, pp. 131–142.
Narayanan, K., Huang, C., Lokugamage, K., Kamitani, W., Ikegami, T., Tseng, C.T., et al., 2008a. Severe acute respiratory syndrome coronavirus nsp1 suppresses host gene expression, including that of type I interferon, in infected cells. J. Virol. 82, 4471–4479.
Narayanan, K., Huang, C., Makino, S., 2008b. Coronavirus accessory proteins. In: - Perlman, S., Gallagher, T., Snijder, E.J. (Eds.), Nidoviruses. ASM Press, Washington, DC, pp. 235–244.
Nga, P.T., Parquet Mdel, C., Lauber, C., Parida, M., Nabeshima, T., Yu, F., et al., 2011. Discovery of the first insect nidovirus, a missing evolutionary link in the emergence of the largest RNA virus genomes. PLoS Pathog. 7, e1002215.
Nugent, C.I., Johnson, K.L., Sarnow, P., Kirkegaard, K., 1999. Functional coupling between replication and packaging of poliovirus replicon RNA. J. Virol. 73, 427–435.
Oostra, M., te Lintelo, E.G., Deijs, M., Verheije, M.H., Rottier, P.J., de Haan, C.A., 2007. Localization and membrane topology of coronavirus nonstructural protein 4: involvement of the early secretory pathway in replication. J. Virol. 81, 12323–12336.
Oostra, M., Hagemeijer, M.C., van Gent, M., Bekker, C.P., te Lintelo, E.G., Rottier, P.J., et al., 2008. Topology and membrane anchoring of the coronavirus replication complex: not all hydrophobic domains of nsp3 and nsp6 are membrane spanning. J. Virol. 82, 12392–12405.
Pan, J., Peng, X., Gao, Y., Li, Z., Lu, X., Chen, Y., et al., 2008. Genome-wide analysis of protein-protein interactions and involvement of viral proteins in SARS-CoV replication. PLoS One 3, e3299.

Pasternak, A.O., Spaan, W.J.M., Snijder, E.J., 2006. Nidovirus transcription: how to make sense…? J. Gen. Virol. 87, 1403–1421.
Penzes, Z., Tibbles, K., Shaw, K., Britton, P., Brown, T.D., Cavanagh, D., 1994. Characterization of a replicating and packaged defective RNA of avian coronavirus infectious bronchitis virus. Virology 203, 286–293.
Penzes, Z., Wroe, C., Brown, T.D., Britton, P., Cavanagh, D., 1996. Replication and packaging of coronavirus infectious bronchitis virus defective RNAs lacking a long open reading frame. J. Virol. 70, 8660–8668.
Qu, H.L., Michot, B., Bachellerie, J.P., 1983. Improved methods for structure probing in large RNAs: a rapid 'heterologous' sequencing approach is coupled to the direct mapping of nuclease accessible sites. Application to the 5′ terminal domain of eukaryotic 28S rRNA. Nucleic Acids Res. 11, 5903–5920.
Raman, S., Brian, D.A., 2005. Stem-loop IV in the 5′ untranslated region is a cis-acting element in bovine coronavirus defective interfering RNA replication. J. Virol. 79, 12434–12446.
Raman, S., Bouma, P., Williams, G.D., Brian, D.A., 2003. Stem-loop III in the 5′ untranslated region is a cis-acting element in bovine coronavirus defective interfering RNA replication. J. Virol. 77, 6720–6730.
Ricagno, S., Egloff, M.P., Ulferts, R., Coutard, B., Nurizzo, D., Campanacci, V., et al., 2006. Crystal structure and mechanistic determinants of SARS coronavirus nonstructural protein 15 define an endoribonuclease family. Proc. Natl. Acad. Sci. U.S.A. 103, 11892–11897.
Sawicki, S.G., Sawicki, D.L., 1995. Coronaviruses use discontinuous extension for synthesis of subgenome-length negative strands. Adv. Exp. Med. Biol. 380, 499–506.
Sawicki, S.G., Sawicki, D.L., 1998. A new model for coronavirus transcription. Adv. Exp. Med. Biol. 440, 215–219.
Sawicki, D., Wang, T., Sawicki, S., 2001. The RNA structures engaged in replication and transcription of the A59 strain of mouse hepatitis virus. J. Gen. Virol. 82, 385–396.
Sawicki, S.G., Sawicki, D.L., Siddell, S.G., 2007. A contemporary view of coronavirus transcription. J. Virol. 81, 20–29.
Schelle, B., Karl, N., Ludewig, B., Siddell, S.G., Thiel, V., 2005. Selective replication of coronavirus genomes that express nucleocapsid protein. J. Virol. 79, 6620–6630.
Schreiber, S.S., Kamahora, T., Lai, M.M., 1989. Sequence analysis of the nucleocapsid protein gene of human coronavirus 229E. Virology 169, 142–151.
Scobey, T., Yount, B.L., Sims, A.C., Donaldson, E.F., Agnihothram, S.S., Menachery, V.D., et al., 2013. Reverse genetics with a full-length infectious cDNA of the Middle East respiratory syndrome coronavirus. Proc. Natl. Acad. Sci. U.S.A. 110, 16157–16162.
Sethna, P.B., Hung, S.L., Brian, D.A., 1989. Coronavirus subgenomic minus-strand RNAs and the potential for mRNA replicons. Proc. Natl. Acad. Sci. U.S.A. 86, 5626–5630.
Sethna, P.B., Hofmann, M.A., Brian, D.A., 1991. Minus-strand copies of replicating coronavirus mRNAs contain antileaders. J. Virol. 65, 320–325.
Seybert, A., Hegyi, A., Siddell, S.G., Ziebuhr, J., 2000. The human coronavirus 229E superfamily 1 helicase has RNA and DNA duplex-unwinding activities with 5′-to-3′ polarity. RNA 6, 1056–1068.
Shi, S.T., Lai, M.M., 2005. Viral and cellular proteins involved in coronavirus replication. Curr. Top. Microbiol. Immunol. 287, 95–131.
Shi, S.T., Huang, P., Li, H.P., Lai, M.M., 2000. Heterogeneous nuclear ribonucleoprotein A1 regulates RNA synthesis of a cytoplasmic virus. EMBO J. 19, 4701–4711.
Shi, S.T., Yu, G.Y., Lai, M.M., 2003. Multiple type A/B heterogeneous nuclear ribonucleoproteins (hnRNPs) can replace hnRNP A1 in mouse hepatitis virus RNA synthesis. J. Virol. 77, 10584–10593.

Shien, J.H., Su, Y.D., Wu, H.Y., 2014. Regulation of coronaviral poly(A) tail length during infection is not coronavirus species- or host cell-specific. Virus Genes 49, 383–392.
Smith, C., Heyne, S., Richter, A.S., Will, S., Backofen, R., 2010. Freiburg RNA Tools: a web server integrating INTARNA, EXPARNA and LOCARNA. Nucleic Acids Res. 38, W373–W377.
Smith, E.C., Blanc, H., Surdel, M.C., Vignuzzi, M., Denison, M.R., 2013. Coronaviruses lacking exoribonuclease activity are susceptible to lethal mutagenesis: evidence for proof-reading and potential therapeutics. PLoS Pathog. 9, e1003565.
Smith, E.C., Sexton, N.R., Denison, M.R., 2014. Thinking outside the triangle: replication fidelity of the largest RNA viruses. Annu. Rev. Virol. 1, 111–132.
Snijder, E.J., Bredenbeek, P.J., Dobbe, J.C., Thiel, V., Ziebuhr, J., Poon, L.L., et al., 2003. Unique and conserved features of genome and proteome of SARS-coronavirus, an early split-off from the coronavirus group 2 lineage. J. Mol. Biol. 331, 991–1004.
Snijder, E.J., van der Meer, Y., Zevenhoven-Dobbe, J., Onderwater, J.J., van der Meulen, J., Koerten, H.K., et al., 2006. Ultrastructure and origin of membrane vesicles associated with the severe acute respiratory syndrome coronavirus replication complex. J. Virol. 80, 5927–5940.
Sola, I., Galán, C., Mateos-Gómez, P.A., Palacio, L., Zúñiga, S., Cruz, J.L., et al., 2011a. The polypyrimidine tract-binding protein affects coronavirus RNA accumulation levels and relocalizes viral RNAs to novel cytoplasmic domains different from replication-transcription sites. J. Virol. 85, 5136–5149.
Sola, I., Mateos-Gomez, P.A., Almazan, F., Zuniga, S., Enjuanes, L., 2011b. RNA-RNA and RNA-protein interactions in coronavirus replication and transcription. RNA Biol. 8, 237–248.
Sola, I., Almazan, F., Zuniga, S., Enjuanes, L., 2015. Continuous and discontinuous RNA synthesis in coronaviruses. Annu. Rev. Virol. 2, 265–288.
Spaan, W., Delius, H., Skinner, M., Armstrong, J., Rottier, P., Smeekens, S., et al., 1983. Coronavirus mRNA synthesis involves fusion of non-contiguous sequences. EMBO J. 2, 1839–1844.
Spagnolo, J.F., Hogue, B.G., 2000. Host protein interactions with the 3′ end of bovine coronavirus RNA and the requirement of the poly(A) tail for coronavirus defective genome replication. J. Virol. 74, 5053–5065.
Stammler, S.N., Cao, S., Chen, S.J., Giedroc, D.P., 2011. A conserved RNA pseudoknot in a putative molecular switch domain of the 3′-untranslated region of coronaviruses is only marginally stable. RNA 17, 1747–1759.
Steil, B.P., Barton, D.J., 2009. Cis-active RNA elements (CREs) and picornavirus RNA replication. Virus Res. 139, 240–252.
Stirrups, K., Shaw, K., Evans, S., Dalton, K., Cavanagh, D., Britton, P., 2000. Leader switching occurs during the rescue of defective RNAs by heterologous strains of the coronavirus infectious bronchitis virus. J. Gen. Virol. 81, 791–801.
Su, D., Lou, Z., Sun, F., Zhai, Y., Yang, H., Zhang, R., et al., 2006. Dodecamer structure of severe acute respiratory syndrome coronavirus nonstructural protein nsp10. J. Virol. 80, 7902–7908.
Su, Y.P., Fan, Y.H., Brian, D.A., 2014. Dependence of coronavirus RNA replication on an NH2-terminal partial nonstructural protein 1 in cis. J. Virol. 88, 8868–8882.
Subissi, L., Posthuma, C.C., Collet, A., Zevenhoven-Dobbe, J.C., Gorbalenya, A.E., Decroly, E., et al., 2014. One severe acute respiratory syndrome coronavirus protein complex integrates processive RNA polymerase and exonuclease activities. Proc. Natl. Acad. Sci. U.S.A. 111, E3900–E3909.
Tanaka, T., Kamitani, W., DeDiego, M.L., Enjuanes, L., Matsuura, Y., 2012. Severe acute respiratory syndrome coronavirus nsp1 facilitates efficient propagation in cells through a specific translational shutoff of host mRNA. J. Virol. 86, 11128–11137.

te Velthuis, A.J., Arnold, J.J., Cameron, C.E., van den Worm, S.H., Snijder, E.J., 2010. The RNA polymerase activity of SARS-coronavirus nsp12 is primer dependent. Nucleic Acids Res. 38, 203–214.

Tekes, G., Hofmann-Lehmann, R., Stallkamp, I., Thiel, V., Thiel, H.J., 2008. Genome organization and reverse genetic analysis of a type I feline coronavirus. J. Virol. 82, 1851–1859.

Thiel, V., Herold, J., Schelle, B., Siddell, S.G., 2001. Infectious RNA transcribed in vitro from a cDNA copy of the human coronavirus genome cloned in vaccinia virus. J. Gen. Virol. 82, 1273–1281.

Tohya, Y., Narayanan, K., Kamitani, W., Huang, C., Lokugamage, K., Makino, S., 2009. Suppression of host gene expression by nsp1 proteins of group 2 bat coronaviruses. J. Virol. 83, 5282–5288.

Ulferts, R., Ziebuhr, J., 2011. Nidovirus ribonucleases: structures and functions in viral replication. RNA Biol. 8, 295–304.

Ulferts, R., Imbert, I., Canard, B., Ziebuhr, J., 2010. Expression and functions of SARS coronavirus replicative proteins. In: Lal, S.K. (Ed.), Molecular Biology of the SARS-Coronavirus. Springer, Berlin and Heidelberg, pp. 75–98.

van den Born, E., Gultyaev, A.P., Snijder, E.J., 2004. Secondary structure and function of the 5′-proximal region of the equine arteritis virus RNA genome. RNA 10, 424–437.

van den Born, E., Posthuma, C.C., Gultyaev, A.P., Snijder, E.J., 2005. Discontinuous subgenomic RNA synthesis in arteriviruses is guided by an RNA hairpin structure located in the genomic leader region. J. Virol. 79, 6312–6324.

van den Worm, S.H., Eriksson, K.K., Zevenhoven, J.C., Weber, F., Zust, R., Kuri, T., et al., 2012. Reverse genetics of SARS-related coronavirus using vaccinia virus-based recombination. PLoS One 7, e32857.

van der Most, R.G., Bredenbeek, P.J., Spaan, W.J., 1991. A domain at the 3′ end of the polymerase gene is essential for encapsidation of coronavirus defective interfering RNAs. J. Virol. 65, 3219–3226.

van Hemert, M.J., van den Worm, S.H., Knoops, K., Mommaas, A.M., Gorbalenya, A.E., Snijder, E.J., 2008. SARS-coronavirus replication/transcription complexes are membrane-protected and need a host factor for activity in vitro. PLoS Pathog. 4, e1000054.

Vijay, R., Perlman, S., 2016. Middle East respiratory syndrome and severe acute respiratory syndrome. Curr. Opin. Virol. 16, 70–76.

von Brunn, A., Teepe, C., Simpson, J.C., Pepperkok, R., Friedel, C.C., Zimmer, R., et al., 2007. Analysis of intraviral protein-protein interactions of the SARS coronavirus ORFeome. PLoS One 2, e459.

Wang, Y., Zhang, X., 1999. The nucleocapsid protein of coronavirus mouse hepatitis virus interacts with the cellular heterogeneous nuclear ribonucleoprotein A1 in vitro and in vivo. Virology 265, 96–109.

Wang, Y., Zhang, X., 2000. The leader RNA of coronavirus mouse hepatitis virus contains an enhancer-like element for subgenomic mRNA transcription. J. Virol. 74, 10571–10580.

Wathelet, M.G., Orr, M., Frieman, M.B., Baric, R.S., 2007. Severe acute respiratory syndrome coronavirus evades antiviral signaling: role of nsp1 and rational design of an attenuated strain. J. Virol. 81, 11620–11633.

Weiss, B., Levis, R., Schlesinger, S., 1983. Evolution of virus and defective-interfering RNAs in BHK cells persistently infected with Sindbis virus. J. Virol. 48, 676–684.

Will, S., Reiche, K., Hofacker, I.L., Stadler, P.F., Backofen, R., 2007. Inferring noncoding RNA families and classes by means of genome-scale structure-based clustering. PLoS Comput. Biol. 3, e65.

Will, S., Joshi, T., Hofacker, I.L., Stadler, P.F., Backofen, R., 2012. LocARNA-P: accurate boundary prediction and improved detection of structural RNAs. RNA 18, 900–914.
Williams, A.K., Wang, L., Sneed, L.W., Collisson, E.W., 1993. Analysis of a hypervariable region in the 3′ non-coding end of the infectious bronchitis virus genome. Virus Res. 28, 19–27.
Williams, G.D., Chang, R.Y., Brian, D.A., 1999. A phylogenetically conserved hairpin-type 3′ untranslated region pseudoknot functions in coronavirus RNA replication. J. Virol. 73, 8349–8355.
Woo, K., Joo, M., Narayanan, K., Kim, K.H., Makino, S., 1997. Murine coronavirus packaging signal confers packaging to nonviral RNA. J. Virol. 71, 824–827.
Woo, P.C., Lau, S.K., Chu, C.M., Chan, K.H., Tsoi, H.W., Huang, Y., et al., 2005. Characterization and complete genome sequence of a novel coronavirus, coronavirus HKU1, from patients with pneumonia. J. Virol. 79, 884–895.
Wu, H.Y., Ozdarendeli, A., Brian, D.A., 2006. Bovine coronavirus 5′-proximal genomic acceptor hotspot for discontinuous transcription is 65 nucleotides wide. J. Virol. 80, 2183–2193.
Wu, H.Y., Ke, T.Y., Liao, W.Y., Chang, N.Y., 2013. Regulation of coronaviral poly(A) tail length during infection. PLoS One 8, e70548.
Wu, H.Y., Guan, B.J., Su, Y.P., Fan, Y.H., Brian, D.A., 2014. Reselection of a genomic upstream open reading frame in mouse hepatitis coronavirus 5′-untranslated-region mutants. J. Virol. 88, 846–858.
Xiao, Y., Ma, Q., Restle, T., Shang, W., Svergun, D.I., Ponnusamy, R., et al., 2012. Nonstructural proteins 7 and 8 of feline coronavirus form a 2:1 heterotrimer that exhibits primer-independent RNA polymerase activity. J. Virol. 86, 4444–4454.
Xu, L., Khadijah, S., Fang, S., Wang, L., Tay, F.P., Liu, D.X., 2010. The cellular RNA helicase DDX1 interacts with coronavirus nonstructural protein 14 and enhances viral replication. J. Virol. 84, 8571–8583.
Yang, D., Liu, P., Giedroc, D.P., Leibowitz, J., 2011. Mouse hepatitis virus stem-loop 4 functions as a spacer element required to drive subgenomic RNA synthesis. J. Virol. 85, 9199–9209.
Yang, D., Liu, P., Wudeck, E.V., Giedroc, D.P., Leibowitz, J.L., 2015. SHAPE analysis of the RNA secondary structure of the Mouse Hepatitis Virus 5′ untranslated region and N-terminal nsp1 coding sequences. Virology 475, 15–27.
Yount, B., Curtis, K.M., Baric, R.S., 2000. Strategy for systematic assembly of large RNA and DNA genomes: transmissible gastroenteritis virus model. J. Virol. 74, 10600–10611.
Yount, B., Curtis, K.M., Fritz, E.A., Hensley, L.E., Jahrling, P.B., Prentice, E., et al., 2003. Reverse genetics with a full-length infectious cDNA of severe acute respiratory syndrome coronavirus. Proc. Natl. Acad. Sci. U.S.A. 100, 12995–13000.
Zaki, A.M., van Boheemen, S., Bestebroer, T.M., Osterhaus, A.D., Fouchier, R.A., 2012. Isolation of a novel coronavirus from a man with pneumonia in Saudi Arabia. N. Engl. J. Med. 367, 1814–1820.
Zhai, Y., Sun, F., Li, X., Pang, H., Xu, X., Bartlam, M., et al., 2005. Insights into SARS-CoV transcription and replication from the structure of the nsp7-nsp8 hexadecamer. Nat. Struct. Mol. Biol. 12, 980–986.
Zhang, X., Lai, M.M., 1995. Interactions between the cytoplasmic proteins and the intergenic (promoter) sequence of mouse hepatitis virus RNA: correlation with the amounts of subgenomic mRNA transcribed. J. Virol. 69, 1637–1644.
Zhang, X., Liao, C.L., Lai, M.M., 1994. Coronavirus leader RNA regulates and initiates subgenomic mRNA transcription both in trans and in cis. J. Virol. 68, 4738–4746.
Ziebuhr, J., 2008. Coronavirus replicative proteins. In: Perlman, S., Gallagher, T., Snijder, E.J. (Eds.), Nidoviruses. ASM Press, Washington, DC, pp. 65–81.

Ziebuhr, J., Snijder, E.J., 2007. The coronavirus replicase gene: special enzymes for special viruses. In: Thiel, V. (Ed.), Coronaviruses—Molecular and Cellular Biology. Caister Academic Press, Norfolk, UK, pp. 33–63.
Ziebuhr, J., Herold, J., Siddell, S.G., 1995. Characterization of a human coronavirus (strain 229E) 3C-like proteinase activity. J. Virol. 69, 4331–4338.
Ziebuhr, J., Snijder, E.J., Gorbalenya, A.E., 2000. Virus-encoded proteinases and proteolytic processing in the Nidovirales. J. Gen. Virol. 81, 853–879.
Ziebuhr, J., Thiel, V., Gorbalenya, A.E., 2001. The autocatalytic release of a putative RNA virus transcription factor from its polyprotein precursor involves two paralogous papain-like proteases that cleave the same peptide bond. J. Biol. Chem. 276, 33220–33232.
Zumla, A., Hui, D.S., Perlman, S., 2015. Middle East respiratory syndrome. Lancet 386, 995–1007.
Zúñiga, S., Sola, I., Alonso, S., Enjuanes, L., 2004. Sequence motifs involved in the regulation of discontinuous coronavirus subgenomic RNA synthesis. J. Virol. 78, 980–994.
Zúñiga, S., Sola, I., Moreno, J.L., Sabella, P., Plana-Duran, J., Enjuanes, L., 2007. Coronavirus nucleocapsid protein is an RNA chaperone. Virology 357, 215–227.
Zúñiga, S., Cruz, J.L., Sola, I., Mateos-Gomez, P.A., Palacio, L., Enjuanes, L., 2010. Coronavirus nucleocapsid protein facilitates template switching and is required for efficient transcription. J. Virol. 84, 2169–2175.
Züst, R., Cervantes-Barragan, L., Kuri, T., Blakqori, G., Weber, F., Ludewig, B., et al., 2007. Coronavirus non-structural protein 1 is a major pathogenicity factor: implications for the rational design of coronavirus vaccines. PLoS Pathog. 3, e109.
Züst, R., Miller, T.B., Goebel, S.J., Thiel, V., Masters, P.S., 2008. Genetic interactions between an essential 3′ cis-acting RNA pseudoknot, replicase gene products, and the extreme 3′ end of the mouse coronavirus genome. J. Virol. 82, 1214–1228.